SCHWEIZ. MINERAL. PETROGR. MITT. 80, 225–248, 2000

SHRIMP and IDTIMS U–Pb zircon ages of the pre-Alpine basement in the Internal Western Alps (Savoy and Piemont)

by J.M. Bertrand[1], R.T. Pidgeon[2], J. Leterrier[3], F. Guillot[4], D. Gasquet[3] and M. Gattiglio[5]

Abstract

Conventional and SHRIMP II U–Pb age determinations are reported for orthogneiss zircons from four basement units of the Internal Western Alps, and for detrital zircons from the Belledonne External Crystalline Massif (ECM). The results lead to a reappraisal of the geotectonic evolution of the Penninic basements (Briançonnais and Piemont) and their pre-Alpine origin. Except for the emplacement of the Cogne granodiorite (Valle d'Aosta) dated at 357 ± 24 Ma (conventional IDTIMS analyses) and 356 ± 3 Ma (SHRIMP analyses), little evidence has been found for a Variscan imprint. However, results from the Péclet orthogneiss (482 ± 5 Ma - SHRIMP) and Modane metagranite (452 ± 5 Ma - SHRIMP) in the Sapey gneiss unit, and the Ambin metarhyolite (500 ± 8 Ma - SHRIMP) from the Ambin massif, show that a major plutonic and tectonic event occurred at 450–500 Ma. Evidence has also been found for a major plutonic event of Permian age (269 ± 6 Ma SHRIMP age from the Gran Paradiso orthogneiss) which suggests important Paleotethyan activity at least in the Piemont basement. SHRIMP dating of detrital zircons from a metasediment of the Belledonne massif (ECM) and zircon cores and xenocrysts found in most of the analysed magmatic rocks show a large Pan-African age component (590–630 Ma) in both the External and Internal Alps. This suggests that there is little difference in the composition of the basement between (1) the ECM, which show a clear continuity with Variscan Europe, (2) the Penninic basements, which may represent allochthonous Alpine terranes, and (3) the Southern Alpine and Austro-Alpine domains, classically attributed to an "African" indenter. They all belong to Gondwana but differ strongly in their Variscan and Alpine history.

Keywords: Penninic Alps, Briançonnais, Piemont, zircon, U–Pb geochronology, SIMS.

1. Introduction

In the Western Alps pre-Mesozoic basement massifs are intercalated with Mesozoic cover formations which are used to define contrasting palaeogeographical and structural domains (DEBELMAS and LEMOINE, 1970). Several such domains make up the Internal Alps (Penninic Domain) which are squeezed between the "External" Alps (Helvetic Domain = Dauphinois in France), which represent the European plate margin, and the Southern Alpine Domain in Italy (as well as the Austro-Alpine Domain in Switzerland and Austria), which belongs to an Apulian-Adriatic microplate. The Internal Alps comprise, from west to east, (Figs 1 and 2): (i) the Valaisan Oceanic Zone, which is Late Cretaceous to Eocene in age; (ii) the Briançonnais Zone, which is dominated by pre-Alpine continental crust; (iii) the Ligurian-Piemont Oceanic Zone, which is Early Jurassic to Cretaceous in age and (iv) the Piemont Zone basement massifs and their thin Mesozoic cover, which are completely embedded within Ligurian-Piemont tectonic units.

Seismic profiles and detailed mapping of key areas, especially in the Central Alps, have shown the continuity of these domains (SCHMID et al., 1996) along the entire belt even where tectonic imbrication is complex. The pre-Alpine basement occurring in the Briançonnais and Piemont zones

[1] Laboratoire de Géodynamique des Chaînes Alpines, Université de Savoie, Domaine universitaire, F-73376 Le Bourget-du-Lac Cedex, France. <Jean-Michel.Bertrand@univ-savoie.fr>
[2] School of Applied Geology, Curtin University of Technology, Kent Street, Bentley 6102, WA, Australia.
[3] Centre de Recherches Pétrographiques et Géochimiques, BP20, F-54501 Vandoeuvre-lès-Nancy Cedex, France.
[4] Laboratoire Sédimentologie and Géodynamique, Université des Sciences et Techniques de Lille, F-59655 Villeneuve d'Ascq Cedex, France.
[5] Universita degli studi di Torino, Dipartimento di Scienze della Terra, Via Valperga Caluso 37, I-10125 Torino, Italia.

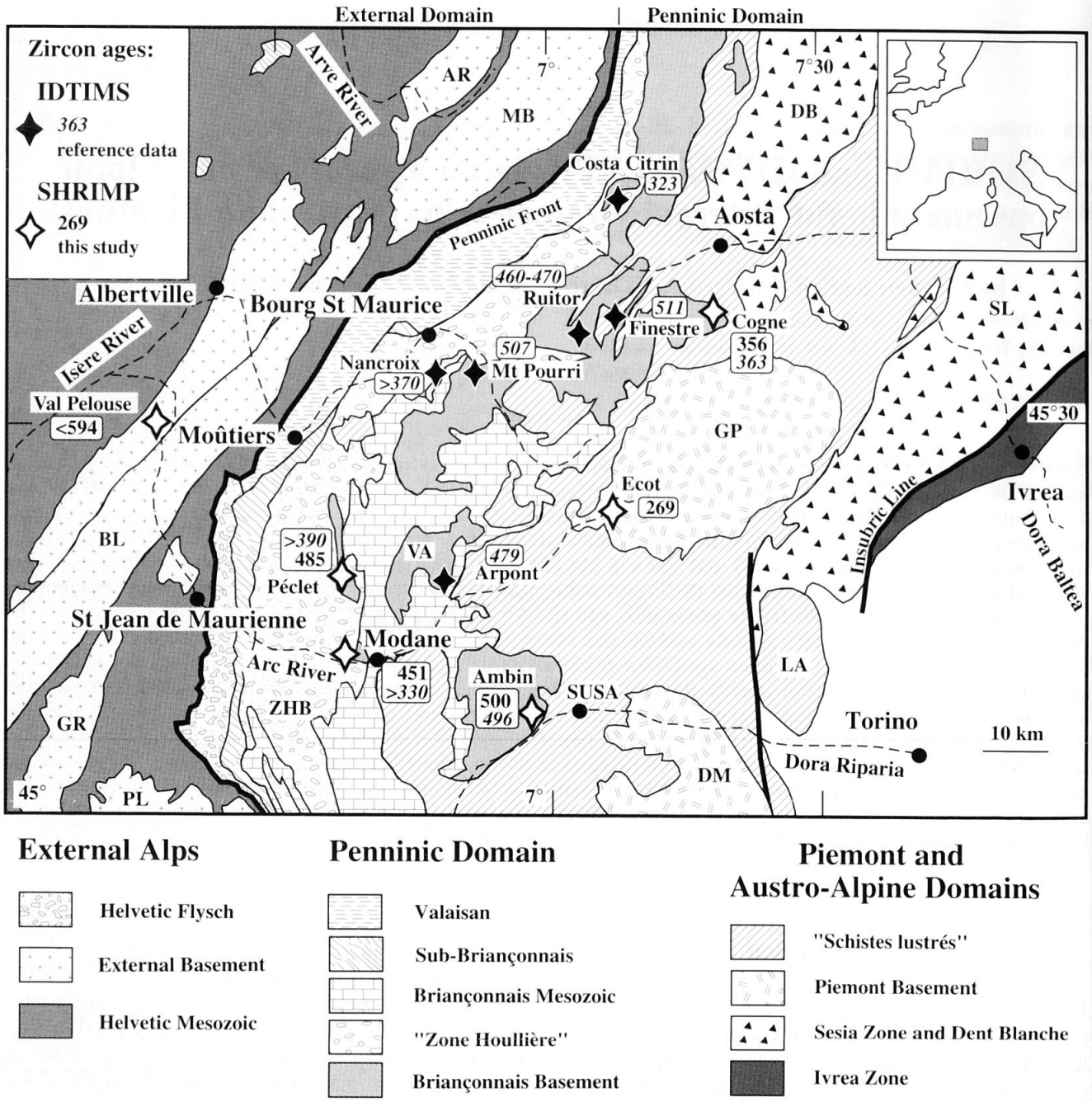

Fig. 1 Sketch map of the study area showing the location of the available U–Pb dates (except for Dora Maira and External Crystalline Massifs). Conventional ages are in italics. AR: Aiguilles Rouges; MB: Mont Blanc; BL: Belledonne; GR: Grandes Rousses; PL: Pelvoux; VA: Vanoise; ZHB: Zone Houillère Briançonnaise; DB: Dent Blanche; GP: Gran Paradiso; SL: Sesia Zone; LA: Lanzo Massif; DM: Dora Maira.

are characterised by strong penetrative structural and metamorphic reworking of Alpine age, including high-pressure metamorphism. The Briançonnais basement comprises mostly metasedimentary formations, some of which have been metamorphosed under low-grade conditions. Some formations contain Carboniferous fossils. Magmatic rock types are rare and this basement has long been considered a metamorphic equivalent to Permo-Carboniferous sediments (ELLENBERGER, 1958). On the contrary, orthogneisses are common in the Piemont basement. They are believed to represent deformed Variscan granitoids (BEARTH, 1952; BERTRAND, 1968; VEARNCOMBE, 1983; BORGHI et al., 1994).

The so-called "stable Europe" which existed before Mesozoic rifting was already a collage of microplates of Gondwanian origin stacked against Baltica (Avalon, Armorica ...) and most of the Variscan belt had already formed at the expense of Gondwanian crust. Several recent papers have tried to reconcile the Early to Late

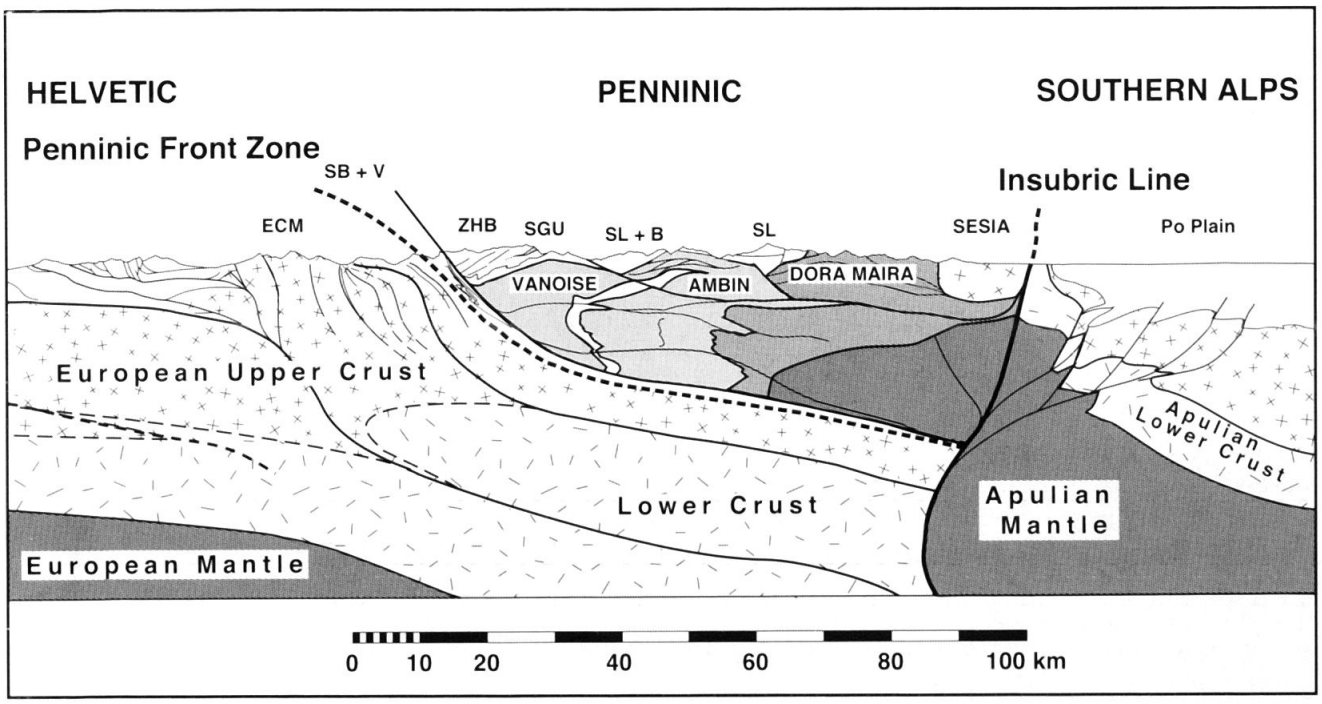

Fig. 2 An interpretative cross-section of the Western Alps along the Arc and Dora Riparia rivers (adapted from a paper in prep.). Four layers are distinguished: mantle = dark grey; lower crust = random dashes; middle crust = random crosses; upper crust = white. In the Penninic domain medium grey ornaments correspond to the different basement units. Abbreviations: ECM = External Crystalline Massifs; SB + V = Sub-Briançonnais and Valaisan Zones; ZHB = Zone Houillère Briançonnaise; SL + B = Piemont Schistes Lustrés and Briançonnais cover; SL = Piemont Schistes Lustrés.

Paleozoic and Mesozoic rifting with pre-Alpine evolution by focussing on the behaviour of the Intra-Alpine terrain as a remnant of the Variscides (VON RAUMER and NEUBAUER, 1993; NEUBAUER and VON RAUMER, 1993; STAMPFLI, 1996; VON RAUMER, 1998; STAMPFLI et al., 1998; SCHALTEGGER and GEBAUER, 1999).

To complement the classical paleogeographical approach, based on the stratigraphy of the Mesozoic cover, we have undertaken a zircon U–Pb geochronological study aimed at investigating the basement rocks for possible Variscan or pre-Variscan signatures. Our objective was to expand the understanding of this lesser-known part of the Variscan belt as a basis for determining the origin of basement rocks found in the Internal Alps.

This paper provides new zircon U–Pb ages of pre-Alpine basement rocks from the Briançonnais and the Piemont zones of the Western Alps, which may help to evaluate their plate origin and possible lateral displacements within the Western Alps (RICOU, 1980; RICOU and SIDDANS, 1986; STAMPFLI, 1993; STAMPFLI et al., 1998). SHRIMP U–Pb data on zircon complement a preliminary conventional TIMS study (BERTRAND et al., 1998) that produced only lower intercept minimum ages. SHRIMP dating has been undertaken on some of the samples previously investigated, albeit unsuccessfully, by conventional techniques. This complements new results obtained using conventional and SHRIMP dating of zircons found in other samples. SHRIMP results are also presented for zircons from a detrital metasediment from the External Crystalline Massifs (ECM), which was chosen as a reference point for the European Variscan crust exposed in the foreland.

2. Geological setting

2.1. GEOLOGICAL SETTING OF THE BRIANÇONNAIS ZONE

The Briançonnais Zone is part of the Penninic Domain which is separated from the Helvetic Domain by the Penninic Front, a major tectonic contact. A summary of the tectonic evolution of the Briançonnais (Figs 1 and 2) and recent syntheses and interpretations, may be found in several papers and references therein (MUGNIER et al., 1993; BERTRAND et al., 1996; CABY, 1996; FÜGENSCHUH et al., 1999). The main differences between the Briançonnais and the External domains include:

– The youngest sediments in the Briançonnais are Lower Eocene in age and the last metamorphic event is dated at ca. 32–35 Ma (e.g. FREEMAN et al., 1997). On the contrary, stratigraphical con-

straints indicate a Miocene low-grade metamorphism in the External Alps. Thus, the External Alps may be considered as a foreland where exhumation of the External Crystalline Massifs is still active, as seen in geodetic measurements and fission track data (SEWARD and MANCKTELOW, 1994; FÜGENSCHUH et al., 1999).

– The stratigraphical record of the Briançonnais formations shows a thick Namurian to Stephanian sequence of low metamorphic grade (the "Zone Houillère Briançonnaise") together with thick Permian and Triassic formations which contrast sharply with the Stephanian basins and the reduced Permian and Triassic formations observed in the External Alps. From Jurassic to Eocene times, the geological record in the different individual nappes forming the Penninic Domain is highly variable.

– A conspicuous reversal of the average dip of the regional foliation is observed on both sides of the Penninic Front. East-dipping structures in the External Alps and in the outer units of the Penninic Domain are in contrast with a dominantly west-dipping to flat-lying foliation in the Briançonnais and the basement domes outcropping further East (Vanoise, Ambin, Gran Paradiso and Dora-Maira domes). The tectonic significance of this foliation fan and of the accompanying East-verging folds are still the object of much discussion (see CABY, 1996). The latest stages of the tectonic evolution correspond to extensional shear zones showing a top-to-the-West movement in the ZHB (AILLÈRES et al., 1995) and a top-to-the-East movement further East in the Ambin dome (GANNE, 1999).

– All the Penninic basement units are strongly reworked and their main foliation is of Alpine age with only some relicts of pre-Alpine structures and/or metamorphic assemblages surviving. This is in contrast to the External Crystalline Massifs, where pre-Alpine structures and metamorphic assemblages are still recognisable and often capped by a Permian unconformity.

2.2. GEOLOGICAL SETTING OF THE PIEMONT AND LIGURIAN-PIEMONT ZONES

The Piemont gneissic domes (Dora-Maira, Gran Paradiso and Monte Rosa) are dominantly of magmatic origin. In the Western Alps, they form the structurally deepest observable units and were affected by high-pressure metamorphism (CHOPIN and MALUSKI, 1980). With their thin and discontinuous cover of highly deformed Mesozoic rocks, they are surrounded by meta-ophiolites, greenstones and calcschists of the Ligurian-Piemont nappes. Their attribution to a subducted equivalent of the European margin (SCHMID et al., 1996; SCHMID and KISSLING, 2000), is discussed by STAMPFLI et al. (1998) who argues that they may correspond to slices of the Apulian plate.

The lowest nappes of the Ligurian-Piemont tectonic pile (FUDRAL, 1998) are dipping West, beneath the Briançonnais Zone. The uppermost nappes form tectonic klippen on top of the Briançonnais, very close to the Penninic Front. Finally, before reaching the Insubric fault and the Ivrea Zone (lower crust of the Southern Alpine Domain), the Sesia Zone represents a high-pressure equivalent of the Austro-Alpine domain.

2.3. PREVIOUS DATING

In the Western Alps, the External Crystalline Massifs comprise huge volumes of either ca. 300 Ma or ca. 340 Ma (in the Mont Blanc and Belledonne-Sept-Laux massifs, respectively) radiometrically dated granites (BUSSY and VON RAUMER, 1994; DEBON et al., 1998), although older ages are known (ca. 500 Ma, MÉNOT et al., 1988a and b; BUSSY and VON RAUMER, 1994). From the Penninic Front eastwards, many of the radiometric studies were concerned primarily with the dating of prominent Alpine events (see HUNZIKER et al., 1992, for a review; GEBAUER and RUBATTO, 1998, for recent developments). Concerning the basement of the Internal Alps, recent U–Pb data favour the presence of Variscan and pre-Variscan metamorphosed basement in the Briançonnais Zone, with ages grouped at 325–330 Ma and around 500 Ma (GUILLOT et al., 1991; BUSSY et al., 1995; BUSSY et al., 1996; BERTRAND and LETERRIER, 1997; BERTRAND et al., 1998; DESMONS et al., 1999; BERTRAND et al., 2000; GUILLOT et al., 2000). Although some authors suggested that the Briançonnais Zone was accreted to the European plate after the Variscan events (GUILLOT et al., 1993), the publication of some Variscan metamorphic ages, for example a $^{40}Ar/^{39}Ar$ phengite age of 340–360 Ma from Ambin (MONIÉ, 1990) and an U–Pb monazite age of 330 Ma from the Mont Mort metapelites in the Grand Saint Bernard nappe (BUSSY et al., 1996; GIORGIS et al., 1999) raise doubts over this interpretation.

The samples analysed during this study have been chosen to document both the pre-Variscan and the Variscan events in the Western Alps (Fig. 1). The Sapey gneisses (Péclet, Modane), the Cogne metadiorites and metagranodiorites, and the Ambin metarhyolites belong to the Briançonnais basement and are compared with previously dated samples at ca. 500 Ma (Mont Pourri, Arpont

Tab. 1 U–Pb conventional data. Labels correspond to the size of the analysed fractions: A = > 150 μm; B = 150–100 μm; C = 100–75 μm; D = < 75 μm. Abbreviations: ab. = abraded fraction; nab. = unabraded; euh. = euhedral; viol. = lilac color; br. = brown; Incol. = colourless; yel. = yellow; nedl. = needle-shaped.

	Magnetism	Zircon type	Weight mg	U ppm	Pb* ppm	206Pb / 204Pb error %	206Pb* / 238U error %	207Pb* / 235U error %	207Pb* / 206Pb* error %	Cor x/y	R8 age	R5 age	7/6 age
COGNE - ZH 95 20													
B0	Nm -2° 3.5A	nab. euh. viol. L/l=2 to 3	0.14	645	36	263(0.20)	0.05079(0.29)	0.42450(0.76)	0.06062(0.51)	0.91	319 ± 0.9	359 ± 2.3	626 ± 11
B1	Nm 1°, 3.5A	ab. euh. viol-br. L/l=2 to 3	0.48	684	349	514(0.22)	0.05014(0.18)	0.37319(0.51)	0.05398(0.35)	0.93	315 ± 0.6	322 ± 1.4	370 ± 7
C1	Nm 0°, 3.5A	nab. euh. pink L/l=2 to 3	0.44	1016	50	277(0.27)	0.04945(0.13)	0.36779(0.45)	0.05395(0.34)	0.88	311 ± 0.4	318 ± 1.2	370 ± 9
D1	Nm 0°, 3.5A	nab; euh. pink, limp. L/l=2	0.11	994	48	557(0.30)	0.04750(0.24)	0.35397(0.59)	0.05405(0.38)	0.94	299 ± 0.7	308 ± 0.6	373 ± 9
C2	Nm 0°, 3.5A	nab, euh. nedl. cloud. L/l=4	0.22	876	42	221(0.25)	0.04742(0.22)	0.35310(0.61)	0.05401(0.42)	0.91	299 ± 0.6	307 ± 1.6	371 ± 10
AMBIN - AM 96 4													
C1-1	Nm 1°, 3.5A	nab. euh. Incol. L/l= to >2	0.02	513	26	115(0.10)	0.04558(0.22)	0.34457(0.88)	0.05482(0.72)	0.80	287 ± 0.6	300 ± 2.3	405 ± 28
C1-2	Nm 2°, 3.5A	nab. euh. Incol. L/l= to >2	0.10		19	197(0.30)	U not measured		0.05671(0.88)				480 ± 19
C2-1	Nm 1°, 3.5A	nab. euh. Incol. L/l< to =2	0.01	1519	141	89(0.10)	0.03952(0.32)	0.28610(1.57)	0.05250(1.33)	0.78	250 ± 0.8	255 ± 3.5	307 ± 41
C2-2	Nm 2°, 3.5A	nab. euh. Incol. L/l< to =2	0.07	358	21	204(0.32)	0.03991(0.27)	0.32131(0.80)	0.05839(0.57)	0.89	252 ± 0.7	282 ± 2.0	544 ± 16
B	Nm 2°, 3.5A	nab, euh cloudy, cracks	0.07	391	17	218(0.18)	0.04007(0.20)	0.31300(0.70)	0.05665(0.53)	0.91	253 ± 0.5	276 ± 1.7	478 ± 29
C	Nm 2°, 3.5A	nab, cloudy, L/l = 2	0.11	273	13	223(0.44)	0.04316(0.23)	0.33766(0.71)	0.05674(0.52)	0.86	272 ± 0.6	295 ± 1.8	482 ± 22
C1	Nm 2°, 3.5A	nab, clear, L/l > to = 2	0.11	411	52	104(0.09)	0.07023(0.38)	0.55070(1.10)	0.05687(0.78)	0.89	437 ± 1.6	445 ± 4.0	487 ± 19
GRAN PARADISO - ZH 96 23													
B4	Nm 2°, 1.7A	nab. euh. pink-br. L/l=1	0.24	741	50	932(0.17)	0.06524(0.22)	0.87085(0.41)	0.09681(0.19)	0.98	407 ± 0.9	636 ± 1.9	1563 ± 5
D2	Nm 2°, 1.7A	nab. euh. pink nedl. L/l= to>5	0.35	763	27	246(0.27)	0.03640(0.19)	0.26272(0.57)	0.05234(0.41)	0.90	230 ± 0.4	237 ± 1.2	301 ± 8
B1	Nm 2°, 1.7A	ab. euh. pink-br. L/l=2	0.15	688	30	1413(0.10)	0.04454(0.15)	0.35639(0.31)	0.05803(0.17)	0.99	281 ± 0.3	309 ± 0.8	531 ± 3
A2	Nm 2°, 1.7A	nab euh. pink nedl. L/l=4	0.27	868	34	1607(0.18)	0.04034(0.17)	0.30511(0.34)	0.05486(0.18)	0.98	255 ± 0.4	270 ± 0.8	406 ± 4
GRAN PARADISO - ZH 96 24													
C3	Nm 2°, 1.7A	nab. euh. flat pink L/l=1 to 2	0.25	768	26	518(0.28)	0.03425(0.16)	0.24709(0.49)	0.05232(0.36)	0.89	217 ± 0.3	224 ± 1.0	299 ± 9
D1	Nm 2°, 1.7A	nab. euh. pink L/l=2 to 3	0.24	797	29	355(0.15)	0.03672(0.21)	0.27852(0.56)	0.05501(0.37)	0.93	232 ± 0.5	249 ± 1.2	413 ± 8
D2	Nm 2°, 1.7A	nab. euh. pink nedl. L/l>4	0.19	771	24	1894(0.50)	0.03230(0.12)	0.22827(0.33)	0.05126(0.23)	0.94	205 ± 0.2	209 ± 0.6	253 ± 5
B1	Nm 2°, 1.7A	ab. euh. pink-yel. L/l=2 to 3	0.17	719	34	912(0.64)	0.04856(0.16)	0.41315(0.37)	0.06171(0.23)	0.94	306 ± 0.5	351 ± 1.1	664 ± 7

and Finestre on figure 1: GUILLOT et al., 1991; BERTRAND and LETERRIER, 1997; BERTRAND et al., 2000). The Gran Paradiso orthogneisses (Ecot) belong to the Piemont Zone. The Belledonne micaschists (Val Pelouse) belong to ECM, which represents the Variscan basement of the pre-Alpine European margin.

3. Analytical procedures

Zircon concentrates have been prepared following usual procedures of crushing, sieving and heavy mineral separation. The best quality grains were selected to produce small, homogeneous (size, magnetism and morphology) fractions for conventional analyses. Epoxy mounts for SHRIMP analysis were prepared with a mixture of the best zircon grains together with more complex, zoned crystals to date inheritance. Preliminary BSEM imaging was performed in all cases to study the internal characteristics of the zircon grains. Microscope photographs (reflected and transmitted light) were used to determine the location of spots in the grains. After the SHRIMP session, further BSEM imaging of the analysed mounts was undertaken to check the quality of the analysed craters and their significance (Fig. 3).

To describe the internal structure of complex zircons, three types of domains have been defined and are used in the following descriptions: Z = zoned domains corresponding to regularly zoned parts of grains. In most cases they are localised at the tips of elongate euhedral grains; they are believed to represent crystal growth during magmatic crystallisation; H = homogeneous domains; C = central part of grains, which in some cases represent inherited cores but often show a nebulitic texture, the significance of which is still unclear.

3.1. CONVENTIONAL ANALYSES (IDTIMS)

Zircon fractions < 0.5 mg were digested following the procedure of PARRISH (1987). Uranium and lead were separated using anion exchange techniques following the method of KROGH (1973). A mixed $^{235}U/^{208}Pb$ spike was used and common lead blanks, determined for each batch of seven fractions, varied between 27 pg and 97 pg. Pb (Rh filament) and U (W filament) were analysed on a Cameca 206 mass spectrometer. Errors are given at the 95% confidence level and take into account the uncertainty on the measured ratios, common lead (procedural blank and STACEY and KRAMERS' correction, 1975) and the mass discrimina-

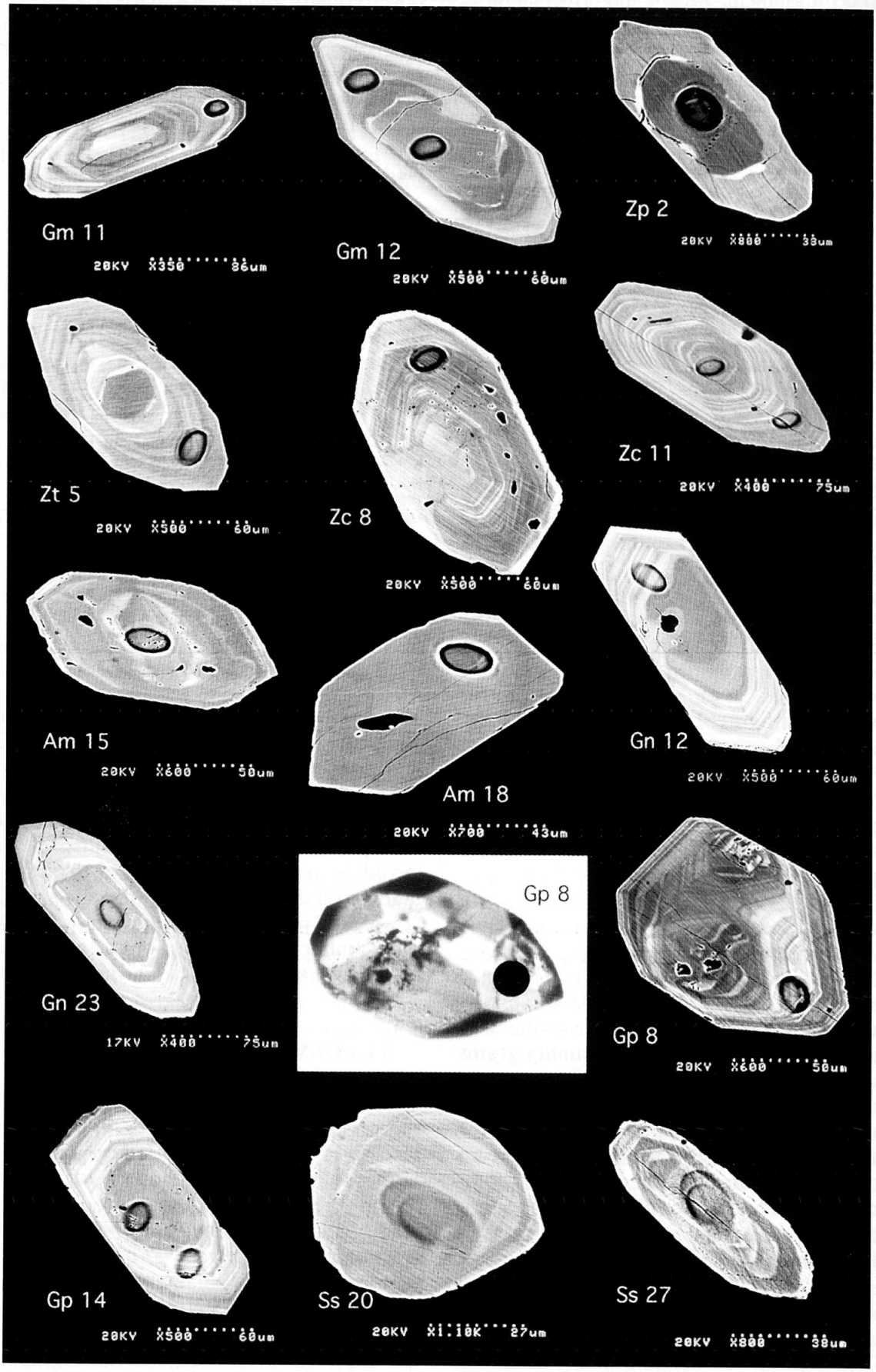
Gm 11
Gm 12
Zp 2
Zt 5
Zc 8
Zc 11
Am 15
Am 18
Gn 12
Gn 23
Gp 8
Gp 8
Gp 14
Ss 20
Ss 27

Fig. 3

tion estimated from the repeated analyses of a standard (NBS 983) for each batch of seven fractions. Regression lines and ages have been calculated using Isoplot (LUDWIG, 1999). Analytical data are given in table 1.

3.2. SHRIMP ANALYSES

The procedures used for the SHRIMP II analyses at Curtin University are described in detail by NELSON (1997). The gem zircon (Cz3) used as a standard (PIDGEON et al., 1994; NELSON, 1997) has an age of 564 Ma and a U concentration of 530–560 ppm. Errors are expressed as 1σ in tables and figures and are given at the 95% confidence level for ages presented in the text. Data were reduced following the method of NELSON (1997). Lead/Uranium ratios are determined relative to that of the Cz3 standard, which has a $^{206}Pb/^{238}U$ value of 0.0914. The SHRIMP Pb/U data were normalised using a power law relating Pb*/U and UO/U with the exponent equal to 2 (CLAOUÉ-LONG et al., 1995). Decay constants used in all dating methods employed in this paper are those recommended by STEIGER and JÄGER (1977). The common lead correction was made using the ^{204}Pb correction method (COMPSTON et al., 1984), using the Broken Hill lead isotopic composition. Points with a $^{206}Pb/^{204}Pb$ ratio < 1000 were neglected in the age estimates as they correspond to spots where microcracks or altered zones were observed under SEM during a later survey.

SHRIMP analyses were performed by alternating analyses of the sample and the standard (one standard for each three samples) to allow monitoring of Pb^+/U^+ discrimination. A detailed table of the measured standard values is available on request. To determine the parameters used for data reduction, the best fit line on the diagram *ln* Pb*/U vs *ln* UO/U was calculated either separately, as for samples G94004, ZH 96 23, ZH 94 2, SS 97 15, or grouped for a one-day session (ZH 95 19 + ZH 96 24 and AM 96 6 + part of ZH 94 2). Sample ZH 94 2 is a special case, as analytical problems occurred during the first session leading to an insufficient number of points and standards. Subsequently, the two groups of data for this sample have been reduced separately. Another special case is sample SS 97 15 (detrital zircons) where only 4 scans were performed for each analysis in order to obtain more (but less precise) data. Concerning Phanerozoic ages, $^{206}Pb/^{238}U$ ages are preferred as discussed in detail and recommended by CLAOUÉ-LONG et al. (1995). Analytical data are given in table 2.

4. Geochronological results

4.1. THE SAPEY GNEISS UNIT (SGU)

The SGU discontinuously marks the eastern edge of the low-grade "Zone Houillère Briançonnaise". The contact is interpreted either, as a major detachment zone according to extension-dominated models (CABY, 1996) or, as a refolded thrust contact (AILLÈRES et al., 1995; BERTRAND

Fig. 3 Selected BSEM images. *Modane:* Gm 11 – Euhedral zircon, the left tip showing an incipient corrosion. Thick regularly zoned domain, the central part being less defined, with rounded and nebulitic zoning (spot in the zoned domain). Gm 12 – Euhedral zircon showing a thin unzoned external domain. The central domain comprises a grey homogeneous part with white discontinuous zones and quartz micro-inclusions and an intermediate part where zoning is nebulitic (spot 1 is in the intermediate, nebulitic area; spot 2 in the homogeneous center). *Péclet:* Zp 2 – Euhedral zircon with curved faces suggesting a metamorphic crystallisation or resorption. Two domains are sharply separated by an altered zone and cracks (spot in the homogeneous core). Zt 5 – Euhedral zircon showing an obvious core and a large regularly zoned domain. Whitened zone at the contact core-zoned domain (spot in the zoned domain). *Cogne:* Zc 8 – Subhedral to euhedral zircon grain showing three different domains: a regularly zoned, dark, central domain surrounded by a lighter external domain mostly developed on the subhedral tip; a third, unzoned domain cross-cuts the previous one but may be in continuity with the external domain (spot in the zoned domain). Zc 11 – Euhedral regularly zoned zircon. The central part is darker and more nebulous (spot 1 is near the tip and cut by a large crack; spot 2 is in the central part). *Ambin:* Am 15 – Euhedral zircon showing netlaced faces. Zoning is nebulitic and the central domain is altered (spot in the central domain, with many quartz micro-inclusions). Am 18 – Euhedral unzoned zircon. *Gran Paradiso:* Gn 12 – Euhedral zircon showing netlace development on the right tip. Obvious grey core with curved contacts; the external domain is regularly zoned (spot in the zoned domain). Gn 23 – Euhedral fractured zircon with a well-defined core. The thick external domain is zoned, sometimes nebulitic (spot in the core showing a blind micro-crack). Gp 8 – Euhedral zircon (optical microscope image). A regularly zoned external domain is sharply discordant to the complexly zoned core, locally altered with quartz exsolution (spot in the central domain). Gp 14 – Euhedral zircon showing an obvious core, slightly altered (quartz exsolution). A thick zoned domain is similarly altered (spot 1 in the zoned domain but in an area with quartz micro-inclusions; spot 2 in the central domain with micro-inclusions). *Val Pelouse:* Ss 20 – Rounded detrital grain almost homogeneous. Ss 27 – Rounded zoned zircon, the core of which yielded the oldest age found in the sample.

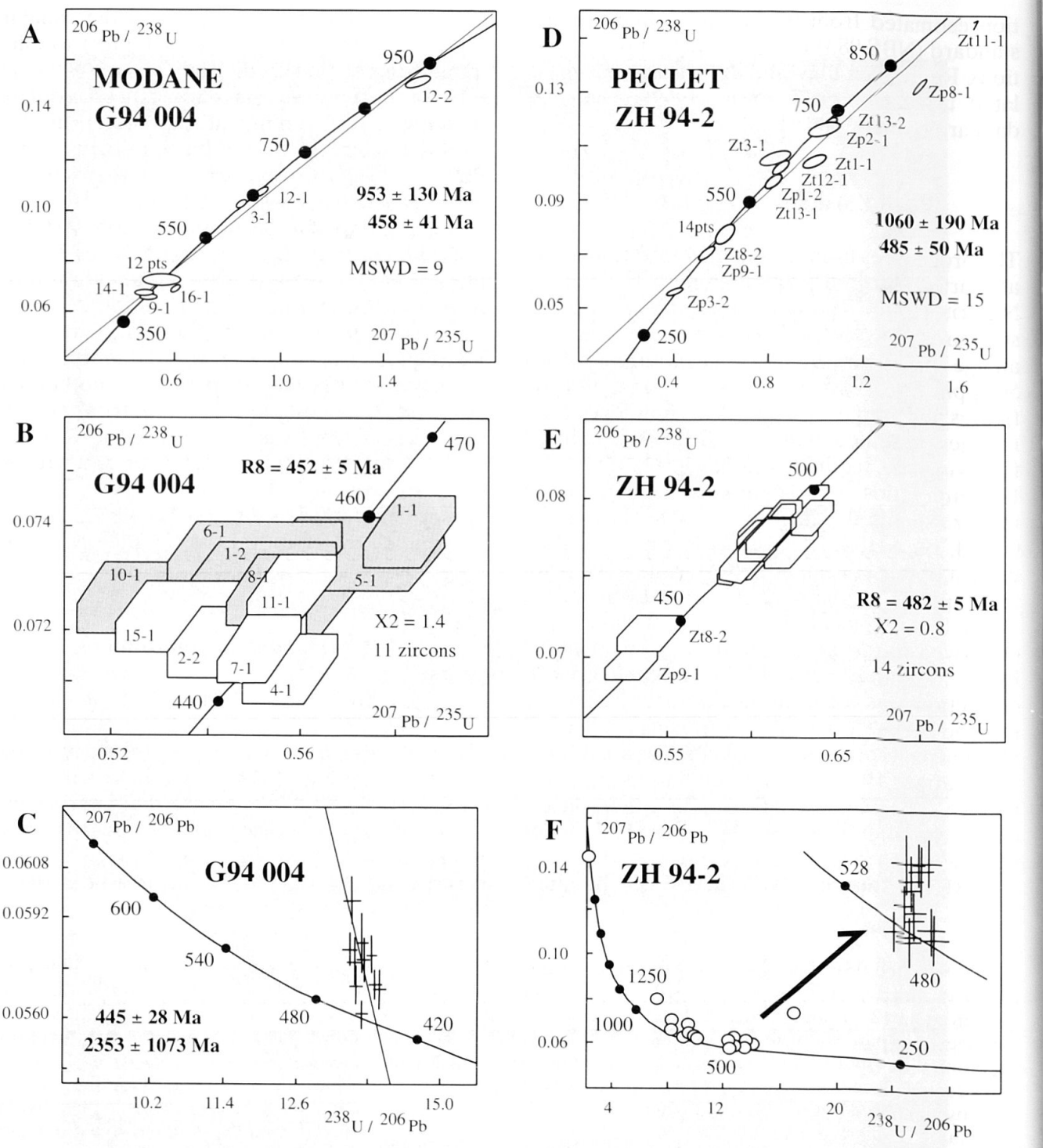

Fig. 4 Concordia diagrams for Modane porphyritic granite and Péclet orthogneiss (SHRIMP data, 1σ errors): (A) Modane G94 004 SHRIMP data; (B) enlargment of the 11 concordant points (filled boxes = cores); (C) Tera-Wasserburg diagram for G94 004 sample; (D) Péclet ZH 94-2 SHRIMP data, except the oldest inherited point at 2400 Ma; (E) enlargment of the ca. 500 Ma group; (F) Tera-Wasserburg diagram for ZH 94-2 sample.

et al., 1996). Similar basement tectonic lenses mark out this contact towards the North, such as the Ruitor massif (dating in progress) and similar units in Valle d'Aosta and Switzerland. A pre-Alpine metamorphic event is inferred by relict kyanite in metasediments (DÉTRAZ, 1984), but Alpine retrograde assemblages and/or high-pressure overprints are always present.

Previous conventional dating of 3 zircon populations from 3 different orthogneisses (BERTRAND et al., 1998) yielded poorly constrained lower intercept ages of >360 Ma, which indicate a minimum age and a large amount of inherited zircon. Their BSEM images showed that many zircon grains contain an inherited core and a regularly zoned outer rim. Two of the three samples

were selected for the SHRIMP study. Sample G94 004 (West of Modane) is a recrystallised but slightly deformed phorphyritic granite comprising albitised K-feldspar, globular quartz, muscovite and chloritised biotite. Sample ZH 94-2 (Aiguille de Péclet) is a strongly deformed orthogneiss with associated meta-aplites where perthitic K-feldspar forms clasts and biotite is completely replaced by chlorite, titanite and hematite. Zircon morphological types observed in these two samples suggest a calc-alkaline affinity (PUPIN, 1980). Zircon grains from the orthogneiss sample have slightly rounded edges, resulting from either the Alpine deformation or a complex pre-Alpine metamorphic evolution.

The Modane porphyritic granite – Results of 18 SHRIMP analyses performed on zircons from sample G94 004 are shown in table 2 and on figure 4. $^{206}Pb/^{204}Pb$ ratios are high except for three analyses (9-1, 13-1, 14-1). Three analyses have old ages (3-1, 12-1, 12-2). Only one of these (12-2) is located on a well-identified core, its external, zoned domain, being almost concordant at 660 Ma ($^{206}Pb/^{238}U$ age). A fourth analysis (16-1) also appears to be inherited and yields a $^{207}Pb/^{206}Pb$ age of ca. 600 Ma. The main group of concordant analytical points (Fig. 4b) comprises 11 analyses corresponding to zoned (Z) domains (5 analyses) and to poorly contrasted, often nebulitic, cores (C). Analytical points of core domains are slightly above concordia and are clearly separated from the Z points. The better concordancy of the Z domains would support the choice of their $^{206}Pb/^{238}U$ average age (448 ± 6Ma) as the best estimate for the magmatic crystallisation of the Sapey zircons but this age is not significantly different from an estimate made by pooling all 11 points giving: $^{206}Pb/^{238}U$ age = 452 ± 5 Ma ($X^2 = 1.37$); $^{207}Pb/^{235}U$ age = 450 ± 6 Ma ($X^2 = 0.93$); $^{207}Pb/^{206}Pb$ age = 443 ± 26 Ma ($X^2 = 0.89$). The most concordant point (8-1) yields a $^{206}Pb/^{238}U$ age of 454 Ma. On a TERA and WASSERBURG (1974) diagram (Fig. 4c), where data are not corrected for common lead (common Pb uncorrected data are available on request), the main group is aligned with a lower intercept at 445 ± 28 Ma. Two points are almost concordant at about 600 Ma (not shown on Fig. 4c) and the upper intercept at about 2500 Ma confirm the presence of an inherited component in the zircon population.

The Péclet orthogneiss – Sample (ZH 94-2) was analysed during two different SHRIMP sessions: 4 standards and 11 unknowns; and 8 standards and 15 unknowns. Standard calibrations and data reduction were carried out separately for each set of data but the last statistical treatment was done on the whole set, using an averaged error on the standard line (1.55%) and the total number of analysed standards (21, including standards analysed with the Ambin sample).

Analytical data define three groups on the concordia diagram (Fig. 4d):

(i) Points with apparent ages older than 500 Ma are xenocrysts (Zt 13-1), or well-identified cores. The oldest one (Zt 11-1) is almost concordant at 2400 Ma. Other concordant points are grouped at ca. 720 Ma (group 1) and at ca. 600–650 Ma (group 2). An interesting zircon grain is Zt 13, whose core is discordant at 770 Ma ($^{207}Pb/^{206}Pb$ age), whereas the corresponding tip is almost concordant at 603 Ma ($^{206}Pb/^{238}U$ age). Another point yields a similar $^{206}Pb/^{238}U$ age of 606 Ma (Zp 1-2) and the corresponding tip is part of the younger concordant group (3). A similar pattern is observed for grain Zt 1, whose highly discordant core yields an apparent $^{207}Pb/^{206}Pb$ age of 923 Ma and corresponding zoned (Z) domain is part of the main group (3). Groups 1 and 2 indicate inheritance from at least two different sources.

(ii) The main group (group 3) of concordant points (Fig. 4e) corresponds to 14 zoned (Z) domains which form a very homogeneous cluster: $^{206}Pb/^{238}U$ age = 482 ± 5 Ma ($X^2 = 0.81$); $^{207}Pb/^{235}U$ age = 484 ± 6 Ma ($X^2 = 0.85$); $^{207}Pb/^{206}Pb$ age = 492 ± 15 Ma ($X^2 = 0.65$). The $^{206}Pb/^{238}U$ age is interpreted as the age of primary crystallisation of the granitic protolith.

(iii) Three points are located below the main group (Zp 3-2, Zp 9-1 and Zt 8-2). From SEM examination all these spots are located in zones of secondary alteration associated with micro-inclusions of quartz believed to result from exsolution. These points may be considered as having suffered lead loss.

When plotted on a Tera-Wasserburg diagram (Fig. 4f) the analytical points clearly show two opposite trends on both sides of the 480 Ma group of concordant points. The first trend, from the inherited old zircons converge towards a 600 Ma intercept suggesting a major event at that time and the second corresponds to lead loss from the zoned overgrowths.

4.2. THE COGNE METADIORITE AND METAGRANODIORITES (CD)

This intrusive body is located East (structurally below) of the Ruitor massif, a likely equivalent to the SGU (AMSTUTZ, 1962). The CD forms, in the Cogne valley, the core of the so-called "Valsavaranche backfold" as it both overlies and underlies

Tab. 2 SHRIMP U–Pb isotopic data. Abbreviations: C = central domains (= identified cores in some cases); Z = zoned domains (in most cases = tips of pyramids); H = homogeneous domains; D = detrital grain. nd = not determined.

		U	Th	Th/U	Pb	206Pb/204Pb	207Pb*/206Pb*	206Pb*/238U	207Pb*/235U	208Pb*/232Th	7/6 age	R8 age	R5 age	8/32 age
		ppm	ppm		ppm		±%	±%	±%	±%				
MODANE - Sample G 94 004														
Gm1-1	Z	583	43	0.073	40	15625	0.0573(1.36)	0.0739(0.92)	0.5836(1.72)	0,0246(2.18)	503±30	459±4	467±6	492±30
Gm1-2	C	350	53	0.15	24	6369	0.0548(2.55)	0.0730(0.92)	0.5520(2.82)	0,0222(6.68)	404±57	455±4	446±10	443±29
Gm 2-2	Z	383	156	0.408	28	5181	0.0553(2.44)	0.0718(0.91)	0.5470(2.72)	0,0234(2.53)	424±55	447±4	443±10	468±12
Gm 3-1	Z	994	598	0.602	110	12195	0.0600(0.87)	0.1031(0.91)	0.8531(1.34)	0,0319(1.16)	603±19	633±6	626±6	634±7
Gm 4-1	Z	336	2	0.007	22	83333	0.0568(1.47)	0.0713(0.91)	0.5581(1.83)	0,0308(40.4)	483±33	444±4	450±7	614±244
Gm 5-1	Z	256	27	0.105	18	10309	0.0564(3.06)	0.0735(0.93)	0.5717(3.31)	0,0226(11.5)	470±68	457±4	459±12	451±52
Gm 6-1	Z	252	117	0.463	19	2674	0.0544(3.20)	0.0734(0.93)	0.5502(3.44)	0,0226(2.99)	387±72	457±4	445±12	453±13
Gm 7-1	Z	659	69	0.105	44	10869	0.0558(1.28)	0.0717(0.91)	0.5515(1.66)	0,0217(4.33)	444±28	446±4	446±6	434±19
Gm 8-1	C	998	45	0.045	67	13158	0.0550(1.09)	0.0728(0.91)	0.5525(1.51)	0,0198(8.66)	414±24	453±4	447±7	396±34
Gm 9-1	C	300	455	1.519	28	977	0.0562(4.04)	0.0657(0.94)	0.5091(4.26)	0,0223(1.56)	459±90	410±4	418±15	445±7
Gm 10-1	Z	201	27	0.135	14	3367	0.0541(5.27)	0.0726(0.96)	0.5419(5.47)	0,0199(17.10)	377±119	452±4	440±20	399±68
Gm 11-1	Z	766	59	0.077	52	5848	0.0556(1.32)	0.0728(0.91)	0.5581(1.70)	0,0223(6.12)	438±29	453±4	450±6	445±27
Gm 12-1	Z	471	61	0.129	48	41667	0.0624(0.91)	0.1078(0.92)	0.9276(1.37)	0,0361(2.25)	688±19	660±6	666±7	717±16
Gm 12-2	C	223	81	0.362	35	5682	0.0718(1.46)	0.1519(0.94)	1.5038(1.82)	0,0446(2.31)	980±30	912±8	932±11	881±20
Gm 13-1	Z	175	91	0.52	14	989	0.0564(5.94)	0.0729(0.98)	0.5667(6.14)	0,0233(4.83)	467±132	454±4	456±23	465±22
Gm 14-1	Z	384	103	0.267	27	767	0.0523(4.66)	0.0675(0.95)	0.4868(4.88)	0,0175(8.59)	297±107	421±4	403±16	351±30
Gm 15-1	Z	298	54	0.18	21	3690	0.0540(2.99)	0.0723(0.93)	0.5383(3.38)	0,0208(6.80)	371±67	450±4	437±12	416±28
Gm 16-1	C	674	48	0.071	44	20000	0.0625(1.18)	0.0707(0.91)	0.6095(1.58)	0,0174(7.58)	693±25	440±4	483±6	348±26
PECLET - Sample ZH 94-2														
Zp 1-1	Z	618	29	0.047	44	17857	0.0563(1.29)	0.0777(1.40)	0.6030(2.02)	0,0226(9.49)	465±29	482±6	479±8	453±43
Zp 1-2	C	577	137	0.237	55	33333	0.0603(1.27)	0.0986(1.40)	0.8196(2.00)	0,0300(2.61)	614±27	606±8	608±9	598±15
Zp 2-1	C	57	37	0.651	7	4081	0.0641(5.40)	0.1174(1.47)	1.0385(5.77)	0,0361(4.43)	746±114	716±10	723±30	716±31
Zp 3-1	Z	538	28	0.052	39	7092	0.0567(1.69)	0.0772(1.40)	0.6039(2.32)	0,0240(11.7)	481±37	479±6	480±9	480±56
Zp 3-2	C	486	58	0.12	28	558	0.0519(5.74)	0.0568(1.43)	0.4063(6.08)	0,0179(18.00)	279±132	356±5	346±18	358±64
Zp 4-1	Z	603	35	0.058	44	nd	0.0585(1.44)	0.0788(1.40)	0.6355(2.13)	0,0289(7.75)	548±31	489±7	499±8	576±44
Zp 5-1	C	529	203	0.384	43	nd	0.0575(1.21)	0.0798(1.40)	0.6331(1.96)	0,0277(1.85)	511±27	495±7	498±8	552±10
Zp 6-1	Z	473	43	0.092	35	14286	0.0569(1.64)	0.0779(1.40)	0.6111(2.28)	0,0238(6.57)	488±36	484±7	484±9	476±31
Zp 7-1	Z	557	83	0.149	41	33333	0.0569(1.38)	0.0776(1.40)	0.6093(2.08)	0,0243(3,50)	488±30	482±6	483±8	498±17
Zp 8-1	C	994	27	0.027	128	41666	0.0776(0.56)	0.1341(1.40)	1.4344(1.57)	0,2084(2.27)	1137±11	811±11	903±9	3826±79
Zp 9-1	Z	376	37	0.099	25	4082	0.0551(2.34)	0.0696(1.40)	0.5283(2.87)	0,0197(9.62)	415±52	434±6	431±10	395±38
Zt 1-1	C	136	102	0.745	16	nd	0.0698(3.54)	0.1041(1.71)	1.0022(4.12)	0,0346(3.00)	923±73	638±10	705±21	688±20
Zt 2-1	Z	398	30	0.075	29	12048	0.0569(2.14)	0.0779(1.69)	0.6113(2.89)	0,0236(11.1)	488±47	484±8	484±11	472±52
Zt 3-1	C	77	127	1.651	11	2976	0.0570(6.66)	0.1053(1.74)	0.8272(7.09)	0,0324(2.74)	491±147	645±11	612±33	645±17
Zt 4-1	Z	532	33	0.062	39	45454	0.0563(1.77)	0.0782(1.69)	0.6071(2.59)	0,0252(10.1)	463±39	486±8	482±10	503±50
Zt 5-1	Z	283	40	0.142	21	12195	0.0574(2.24)	0.0785(1.69)	0.6211(2.98)	0,0238(6.24)	506±49	487±8	491±12	475±29
Zt 6-1	C	446	34	0.076	32	nd	0.0586(1.57)	0.0771(1.69)	0.6229(2.44)	0,0252(6.92)	553±34	479±8	492±10	503±34
Zt 7-1	Z	428	23	0.054	30	nd	0.0567(1.15)	0.0758(1.69)	0.5924(2.16)	0,0253(4.17)	479±25	471±8	472±8	505±21
Zt 8-1	Z	576	31	0.053	41	9804	0.0571(1.68)	0.0762(1.69)	0.5998(2.52)	0,0251(10.7)	496±37	473±8	477±10	500±53
Zt 8-2	C	439	9	0.021	29	3030	0.05461(2.84)	0.0716(1.69)	0.5391(3.48)	nd	396±64	446±7	438±12	nd
Zt 9-1	Z	509	15	0.03	36	90909	0.0567(1.62)	0.0761(1.69)	0.5955(2.48)	0,0279(15.5)	481±36	473±8	474±9	556±85
Zt 10-1	Z	734	6	0.008	52	nd	0.0567(0.83)	0.0783(1.69)	0.6124(1.97)	0,0350(6.03)	481±18	486±8	485±8	695±41
Zt 11-1	C	52	39	0.762	27	7092	0.1412(1.48)	0.4504(1.80)	8.7692(2.47)	0,1289(2.81)	2242±26	2397±36	2314±22	2450±65
Zt 12-1	C	205	309	1.507	28	8333	0.0599(2.10)	0.1030(1.69)	0.8510(2.86)	0,0318(1.96)	601±45	632±10	625±13	633±12
Zt 13-1	Z	229	102	0.446	23	nd	0.0601(2.22)	0.0980(1.70)	0.8122(2.95)	0,0317(2.75)	606±48	603±10	604±13	630±17
Zt 13-2	C	256	115	0.447	32	23809	0.0649(1.33)	0.1187(1.69)	1.0612(2.28)	0,0376(2.19)	770±28	723±12	734±12	747±16
COGNE - Sample ZH 95-19														
Zc 2-2	Z	921	301	0.326	53	37000	0.0544(1.27)	0.0577(1.16)	0.4327(1.82)	0.0182(1.87)	387±28	362±4	365±6	365±7
Zc 2-3	Z	354	122	0.345	21	863	0.0512(5.54)	0.0561(1.20)	0.3963(5.81)	0.0176(6.15)	251±128	352±4	339±17	353±22
Zc 3-1	Z	1563	555	0.355	90	23809	0.0533(0.94)	0.0574(1.16)	0.4221(1.58)	0.0175(1.54)	344±21	360±4	358±5	352±5
Zc 4-1	Z	1026	380	0.371	53	12987	0.0544(1.36)	0.0512(1.16)	0.3842(1.90)	0.0155(1.88)	387±31	322±4	330±5	312±6
Zc 5-1	Z	1004	399	0.397	64	588	0.0546(3.56)	0.0565(1.18)	0.4250(3.88)	0.0181(3.92)	394±80	354±4	360±12	364±14
Zc 6-1	Z	826	282	0.341	47	4854	0.0514(1.83)	0.0563(1.17)	0.3992(2.28)	0.0174(2.32)	259±42	353±4	341±7	350±8
Zc 7-1	C	818	229	0.28	43	4504	0.0540(1.89)	0.0530(1.17)	0.3943(2.34)	0.0170(2.77)	371±43	333±4	338±7	341±9
Zc 8-1	Z	353	111	0.316	20	4132	0.0518(3.32)	0.0571(1.17)	0.4080(3.67)	0.0177(4.16)	277±76	358±4	347±11	354±15
Zc 9-1	C	993	329	0.332	56	10204	0.0539(1.50)	0.0558(1.16)	0.4152(2.02)	0.0177(2.07)	368±34	350±4	353±6	356±7
Zc 10-1	Z	847	373	0.44	38	6060	0.0523(1.85)	0.0439(1.17)	0.3168(2.3)	0.0116(2.22)	299±42	277±3	279±6	233±5
Zc 11-1	Z	940	311	0.33	53	2703	0.0531(1.90)	0.0559(1.17)	0.4094(2.34)	0.0176(2.48)	334±43	351±4	348±7	352±9
Zc 11-2	Z	602	202	0.337	34	5747	0.0532(2.41)	0.0566(1.17)	0.4149(2.81)	0.0177(3.00)	336±55	355±4	352±8	354±11
Zc 12-1	C	261	106	0.407	18	375	0.0528(8.98)	0.0557(1.29)	0.4058(9.22)	0.0153(10.50)	320±205	350±4	346±27	307±32
Zc 13-1	Z	1215	474	0.39	71	6024	0.0543(1.46)	0.0572(1.16)	0.4278(1.98)	0.0183(1.87)	383±33	358±4	362±6	366±7
Zc 14-1	C	129	42	0.325	21	4201	0.0715(2.53)	0.1568(1.20)	1.5451(2.93)	0.0467(4.27)	971±52	939±11	949±18	922±38
Zc 15-1	C	772	356	0.462	46	10869	0.0543(1.44)	0.0568(1.16)	0.4256(1.96)	0.0180(1.72)	385±32	356±4	360±6	362±6
Zc 16-1	Z	440	137	0.312	26	3413	0.0532(2.95)	0.0581(1.17)	0.4256(3.31)	0.0181(3.82)	336±67	364±4	360±10	362±14
Zc 17-1	Z	968	305	0.315	48	6536	0.0541(1.76)	0.0488(1.17)	0.3641(2.23)	0.0166(2.32)	373±40	307±4	315±6	332±8

Tab. 2 (cont.) SHRIMP U–Pb isotopic data. Abbreviations: C = central domains (= identified cores in some cases); Z = zoned domains (in most cases = tips of pyramids); H = homogeneous domains; D = detrital grain. nd = not determined.

		U	Th	Th/U	Pb	206Pb/204Pb	207Pb*/206Pb*	206Pb*/238U	207Pb*/235U	208Pb*/232Th	7/6 age	R8 age	R5 age	8/32 age
		ppm	ppm		ppm		±%	±%	±%	±%				
AMBIN - Sample 96 AM 4														
Gm 1-1	H	294	273	0.926	27	6369	0.0563(2.17)	0.0779(1.40)	0.6048(2.72)	0.0.0240(1.86)	465±48	483±7	480±10	479±9
Gm 2-1	H	119	57	0.478	10	2445	0.0528(6.50)	0.0821(1.45)	0.5979(6.83)	0.0.0243(5.86)	320±148	509±7	476±26	485±28
Gm 3-1	H	209	107	0.513	17	38460	0.0591(2.10)	0.0755(1.40)	0.6157(2.66)	0.0.0253(2.27)	572±46	469±6	487±10	505±11
Gm 4-1	H	169	91	0.536	14	7692	0.0561(3.74)	0.0803(1.41)	0.6212(4.16)	0.0.0243(3.38)	455±83	498±7	491±16	486±16
Gm 5-1	H	112	60	0.534	10	432	0.0536(10.60)	0.0780(1.51)	0.5764(10.90)	0.0.0251(7.86)	354±241	484±7	462±40	502±39
Gm 6-1	H	168	86	0.513	14	5319	0.0555(3.36)	0.0809(1.41)	0.6187(3.80)	0.0.0253(3.11)	432±75	501±7	489±15	506±16
Gm 7-1	C	822	182	0.221	30	3145	0.0485(2.45)	0.0371(1.40)	0.2484(2.97)	0.0.0108(4.26)	125±58	235±3	225±6	217±9
Gm 7-2	C	1160	128	0.11	47	200000	0.0514(0.98)	0.0438(1.39)	0.3100(1.80)	0.0.0141(2.51)	257±22	276±4	274±4	282±7
Gm 8-1	H	276	208	0.753	25	21732	0.0575(1.81)	0.0803(1.40)	0.6367(2.42)	0.0.0250(1.88)	510±40	498±7	500±10	500±9
Gm 9-1	H	247	97	0.394	12	2873	0.0558(4.51)	0.0435(1.41)	0.3345(4.89)	0.0.0224(3.32)	443±100	275±4	293±12	448±15
Gm 10-1	H	249	163	0.656	21	2105	0.0566(3.42)	0.0739(1.41)	0.5771(3.86)	0.0.0251(2.57)	476±76	460±6	463±14	501±13
Gm 11-1	H	134	60	0.447	11	8772	0.0564(3.60)	0.0785(1.41)	0.6111(4.03)	0.0.0243(3.71)	470±80	487±7	484±16	485±18
Gm 12-1	H	129	79	0.615	11	7752	0.0584(4.04)	0.0818(1.42)	0.6592(4.45)	0.0.0256(3.29)	546±88	507±7	514±18	512±17
Gm 13-1	H	103	51	0.493	9	850	0.0561(8.82	0.0804(1.49)	0.6224(9.12)	0.0.0249(7.68)	458±196	498±7	491±36	498±38
Gm 14-1	H	110	63	0.571	10	8772	0.0575(4.17)	0.0804(1.42)	0.6368(4.58)	0.0.0257(3.50)	509±92	498±7	500±18	513±18
Gm 15-1	C	316	106	0.336	99	90909	0.1122(0.56)	0.2985(1.41)	4.6169(1.59)	0.0.0929(1.80)	1835±10	1684±21	1752±13	1795±31
Gm 16-1	H	396	258	0.651	35	13889	0.0569(2.32)	0.0807(1.4)	0.6329(2.85)	0.0.0254(1.12)	488±51	500±7	498±11	508±11
Gm 17-1	C	289	119	0.412	179	333333	0.2041(0.29)	0.5445(1.42)	15.3215(1.48)	0.0.1488(1.59)	2859±5	2802±32	2835±14	2804±42
Gm 18-1	H	184	146	0.798	17	4566	0.0549(3.51)	0.0818(1.41)	0.6190(3.94)	0.0.0251(2.46)	407±79	507±7	489±15	501±12
Gm 19-1	H	456	433	0.951	41	19231	0.0570(1.81)	0.0737(1.40)	0.5794(2.42)	0.0.0271(1.66)	493±40	458±6	464±9	540±9
Gm 20-1	H	218	158	0.726	20	6289	0.0572(2.81)	0.0832(1.41)	0.6572(3.29)	0.0.0263(2.28)	501±62	516±7	513±13	526±12
GRAN PARADISO orthogneiss - Sample ZH 96-23														
Gn 1-1	Z	1766	126	0.071	70	10309	0.0523(1.22)	0.0425(1.83)	0.3064(2.32)	0.0.0141(5.19)	299±28	268±5	271±6	283±15
Gn 2-1	C	455	163	0.359	20	5988	0.0519(3.08)	0.0432(1.83)	0.3092(3.73)	0.0.0134(3.69)	283±69	273±5	274±9	270±10
Gn 3-1	C	674	73	0.109	26	3922	0.0498(2.78)	0.0402(1.83)	0.2760(3.52)	0.0.0113(9.70)	184±65	254±5	248±8	227±22
Gn 4-1	C	865	65	0.075	54	8696	0.0585(1.47)	0.0665(1.83)	0.5363(2.49)	0.0.0225(6.84)	550±32	415±7	436±9	450±30
Gn 5-1	Z	653	71	0.109	28	7042	0.0508(2.07)	0.0454(1.83)	0.3181(2.93)	0.0.0131(6.95)	231±48	286±5	280±7	263±18
Gn 6-1	C	1824	402	0.22	65	14493	0.0516(1.36)	0.0368(1.83)	0.2621(2.41)	0.0.0126(2.69)	268±31	233±4	236±5	254±7
Gn 7-1	C	827	35	0.042	33	47619	0.0521(1.67)	0.0433(1.83)	0.3112(2.63)	0.0.0155(10.80)	290±38	273±5	275±6	311±33
Gn 8-1	Z	1171	263	0.225	49	5128	0.0512(1.75)	0.0427(1.83)	0.3013(2.68)	0.0.0125(3.46)	248±40	270±5	267±6	250±9
Gn 9-1	C	287	276	0.961	34	6173	0.0597(1.94)	0.1016(1.83)	0.8373(2.83)	0.0.0314(2.15)	595±42	624±11	618±13	625±13
Gn 10-1	C	419	126	0.301	32	6711	0.0552(2.07)	0.0772(1.83)	0.5878(2.93)	0.0.0230(3.35)	421±46	479±8	469±11	459±15
Gn 11-1	C	329	153	0.464	34	nd	0.0619(1.60)	0.0985(1.83)	0.8410(2.58)	0.0.0310(2.42)	671±34	606±11	620±12	617±15
Gn 12-1	C	1308	99	0.075	51	111111	0.0521(0.92)	0.0420(1.83)	0.3020(2.15)	0.0.0140(2.99)	289±21	266±5	268±5	281±8
Gn 13-1	C	546	187	0.343	24	nd	0.0528(2.86)	0.0434(1.83)	0.3165(3.58)	0.0.0137(3.66)	322±65	274±5	279±9	275±10
Gn 14-1	C	1439	93	0.064	57	40000	0.0510(1.19)	0.0431(1.83)	0.3032(2.31)	0.0.0138(5.61)	242±28	272±5	269±5	277±15
Gn 15-1	C	342	66	0.194	14	3205	0.0491(4.69)	0.0419(1.84)	0.2837(5.25)	0.0.0114(9.90)	153±110	265±5	254±12	229±22
Gn 16-1	C	462	84	0.181	19	9446	0.0514(3.52)	0.0433(1.84)	0.3071(4.17)	0.0.0130(7.55)	261±81	273±5	272±10	261±20
Gn 17-1	C	445	43	0.096	31	nd	0.0580(2.07)	0.0733(1.83)	0.5861(2.92)	0.0.0256(7.56)	530±45	456±8	468±11	511±38
Gn 18-1	C	169	17	0.101	12	47619	0.0604(3.04)	0.0739(1.84)	0.6157(3.74)	0.0.0194(13.64)	620±66	459±8	487±14	389±53
Gn 17-2	C	547	54	0.1	28	nd	0.0579(2.22)	0.0548(1.83)	0.4373(3.05)	0.0.0200(7.18)	525±49	344±6	368±9	400±28
Gn 19-1	C	1205	785	0.652	54	7752	0.0514(1.55)	0.0414(1.83)	0.2932(2.55)	0.0.0123(2.11)	259±36	261±5	261±6	248±5
Gn 20-1	Z	1728	114	0.066	61	25641	0.0520(1.06)	0.0381(1.83)	0.2734(2.22)	0.0.0132(4.44)	287±24	241±4	245±5	265±12
Gn 21-1	C	649	112	0.172	26	8772	0.0516(1.90)	0.0421(1.83)	0.2999(2.80)	0.0.0128(4.16)	270±44	266±5	266±7	257±11
Gn 23-1	C	577	349	0.605	211	24390	0.1159(0.37)	0.3285(1.84)	5.2490(1.92)	0.0.0952(1.91)	1831±29	1893±7	1861±16	1839±34
Gn 24-1	Z	292	120	0.411	12	1381	0.0454(6.74)	0.0401(1.86)	0.2507(7.21)	0.0.0118(6.14)	nd	253±5	227±15	238±15
GRAN PARADISO enclave - Sample ZH 96-24														
Gp1-1	Z	1542	80	0.05	66	5882	0.0501(1.66)	0.0400(1.58)	0.3181(2.15)	0.0.0113(13.00)	202±39	390±3	280±5	227±29
Gp 2-1	C	274	97	0.354	12	2882	0.0545(5.38)	0.0424(1.20)	0.3187(5.66)	0.0.0143(5.76)	391±121	268±3	281±14	288±16
Gp 3-1	C	168	48	0.289	16	5347	0.0613(3.78)	0.0951(1.19)	0.8039(4.11)	0.0.0318(5.52)	649±81	586±7	599±19	633±34
Gp 4-1	C	228	106	0.467	89	15129	0.1290(0.55)	0.3576(1.2)	6.3605(1.38)	0.0.1036(1.55)	2084±10	1971±20	2027±12	1992±29
Gp 5-1	Z	951	107	0.113	38	4807	0.0508(2.18)	0.0421(1.17)	0.2949(2.60)	0.0.0135(6.5)	232±50	266±3	262±6	271±17
Gp 6-1	C	765	514	0.671	82	14706	0.0585(0.92)	0.0977(1.16)	0.7884(1.58)	0.0.0300(1.37)	550±20	601±7	590±7	598±8
Gp 7-1	C	832	233	0.28	35	4926	0.0512(2.19)	0.0424(1.17)	0.2988(2.61)	0.0.0131(3.09)	248±50	267±3	265±6	263±8
Gp 8-1	C	2045	138	0.067	87	22222	0.0511(0.95)	0.0460(1.16)	0.3242(1.59)	0.0.0148(4.01)	248±22	290±3	285±4	297±12
Gp 9-1	C	306	82	0.269	35	4048	0.0627(2.04)	0.1141(1.18)	0.9862(2.48)	0.0.0348(3.57)	697±43	697±8	697±12	691±24
Gp 10-1	Z	1506	184	0.122	59	9009	0.0520(1.33)	0.0418(1.16)	0.2999(1.87)	0.0.0100(4.67)	286±30	264±3	266±4	200±9
Gp 10-2	C	1361	78	0.057	56	8403	0.0511(1.54)	0.0448(1.17)	0.3158(2.05)	0.0.0137(8.78)	247±36	282±3	279±5	276±24
Gp 11-1	C	464	277	0.597	21	3636	0.0520(3.15)	0.0418(1.17)	0.3000(3.49)	0.0.0132(2.45)	286±72	264±3	266±8	264±6
Gp 12-1	C	339	178	0.524	36	5000	0.0600(2.20)	0.0995(1.18)	0.8223(2.62)	0.0.0308(2.26)	602±48	611±7	609±12	614±14
Gp 13-1	C	354	119	0.335	16	1102	0.0484(6.10)	0.0428(1.20)	0.2852(6.36)	0.0.0132(6.66)	117±127	270±3	255±14	265±18
Gp 14-1	Z	1717	126	0.074	66	2681	0.0505(1.74)	0.0406(1.17)	0.2830(2.21)	0.0.0109(9.30)	219±40	257±5	253±5	220±20
Gp 14-2	C	384	167	0.434	154	14925	0.1687(0.39)	0.3579(1.18)	8.3221(1.29)	0.0.1074(1.43)	2544±6	1972±20	226±127	2063±28
Gp 15-1	C	397	120	0.301	38	12345	0.0615(1.50)	0.0964(1.17)	0.8175(2.02)	0.0.0310(2.35)	658±32	593±7	607±9	616±14

Tab. 2 (cont.) SHRIMP U–Pb isotopic data. Abbreviations: C = central domains (= identified cores in some cases); Z = zoned domains (in most cases = tips of pyramids); H = homogeneous domains; D = detrital grain. nd = not determined.

		U	Th	Th/U	Pb	206Pb/204Pb	207Pb*/206Pb*	206Pb*/238U	207Pb*/235U	208Pb*/232Th	7/6 age	R8 age	R5 age	8/32 age
		ppm	ppm		ppm		±%	±%	±%	±%				
VAL PELOUSE - Sample SS 97 15														
Ss 1	D	909	597	0.657	151	4037	0.0695(1.21)	0.1499(2.07)	1.4358(2.52)	0.0457(2.32)	913±25	900±17	904±15	903±20
Ss 2	D	151	59	0.392	21	669	0.0673(6.82)	0.1273(2.14)	1.1810(7.40)	0.0393(8.93)	847±142	772±41	792±41	780±69
Ss 3	D	907	426	0.47	157	6605	0.0732(0.95)	0.1640(2.07)	1.6534(2.38)	0.0494(2.34)	1020±19	979±19	992±15	974±22
Ss 4	D	296	164	0.555	32	883	0.0559(5.50)	0.0980(2.09)	0.7549(6.13)	0.0292(4.85)	448±123	603±12	571±27	582±28
Ss 5	D	433	1884	4.353	529	8192	0.2355(0.35)	0.5884(2.09)	19.1036(2.16)	0.1570(2.13)	3090±6	2983±50	3047±21	2948±58
Ss 6	D	367	798	2.173	89	1789	0.0715(2.13)	0.1592(2.08)	1.5711(3.16)	0.0478(2.24)	973±44	952±18	959±20	944±21
Ss 7	D	249	177	0.71	36	877	0.0615(5.17)	0.1215(2.10)	1.0294(5.82)	0.0387(3.98)	656±111	739±15	719±30	768±30
Ss 8	D	279	232	0.834	33	1153	0.0644(4.26)	0.0988(2.09)	0.8772(4.97)	0.0315(3.30)	755±90	607±12	639±24	628±20
Ss 9	D	175	90	0.51	30	1156	0.0748(3.89)	0.1539(2.11)	1.5884(4.65)	0.0486(4.66)	1064±78	923±18	966±29	958±44
Ss 10	D	210	176	0.84	25	613	0.0590(7.09)	0.0977(2.12)	0.7948(7.65)	0.0291(4.56)	567±155	601±12	594±34	580±26
Ss 11	D	368	452	1.23	47	1390	0.0610(3.70)	0.1007(2.08)	0.8477(4.46)	0.0309(2.64)	640±80	619±12	623±21	615±16
Ss 12	D	1006	131	0.13	98	2941	0.0604(1.77)	0.1010(2.07)	0.8412(2.88)	0.0303(6.05)	619±38	620±12	620±13	604±36
Ss 13	D	153	137	0.9	25	572	0.0609(7.52)	0.1294(2.14)	1.0863(8.07)	0.0385(4.68)	635±162	784±16	747±43	763±35
Ss 14	D	253	176	0.72	47	1562	0.0715(2.80)	0.1614(2.09)	1.5919(3.70)	0.0486(3.12)	973±57	964±19	967±23	960±29
Ss 15	D	145	110	0.76	33	606	0.0696(5.71)	0.1912(2.14)	1.8344(6.34)	0.0535(4.92)	916±118	1128±22	1058±42	1054±51
Ss 16	D	198	75	0.38	22	674	0.0586(6.71)	0.1006(2.11)	0.8131(7.28)	0.0319(7.83)	553±147	618±12	604±33	635±49
Ss 17	D	164	131	0.79	35	990	0.0770(4.02)	0.1767(2.12)	1.8763(4.77)	0.0537(3.76)	1122±80	1049±21	1073±32	1057±39
Ss 18	D	92	89	0.97	20	392	0.0597(9.72)	0.1636(2.20)	1.3468(10.2)	0.0462(5.56)	593±212	977±20	866±60	912±50
Ss 19	D	949	60	0.06	95	2457	0.0602(1.73)	0.1052(2.07)	0.8728(2.86)	0.0275(12.90)	610±37	645±13	637±14	549±70
Ss 20	D	155	158	1.02	21	484	0.0552(10.6)	0.1029(2.16)	0.7834(11.1)	0.0306(5.18)	422±239	631±13	587±50	608±31
Ss 21	D	273	180	0.66	50	1198	0.0685(3.23)	0.1606(2.09)	1.5165(4.06)	0.0472(3.43)	884±67	960±19	937±25	933±31
Ss 22	D	70	7	0.1	8	395	0.0810(11.5)	0.1029(2.30)	1.1492(12.0)	0.0935(23.80)	1222±228	631±14	777±65	1808±412
Ss 23	D	1057	89	0.08	302	5586	0.1354(0.43)	0.2843(2.07)	5.3076(2.17)	0.0664(4.74)	2169±8	1613±30	1870±19	1300±60
Ss 24	D	1068	1052	0.99	114	3125	0.0595(1.67)	0.0897(2.07)	0.7363(2.82)	0.0272(2.26)	585±36	554±11	560±12	543±12
Ss 25	D	212	342	1.6	27	685	0.0605(7.59)	0.0913(2.12)	0.7618(8.13)	0.0270(3.31)	622±164	563±11	575±36	539±18
Ss 26	D	32	17	0.53	6	242	0.0880(16.1)	0.1488(2.63)	1.8055(16.7)	0.0561(16.5)	1382±314	894±22	1047±109	1104±178
Ss 27	D	103	40	0.39	86	3049	0.2925(0.65)	0.6844(2.17)	27.5988(2.35)	0.1789(3.46)	3431±10	3361±57	3405±23	3327±106
Ss 28	D	172	54	0.31	23	687	0.0689(5.79)	0.1236(2.12)	1.1739(6.41)	0.0368(9.88)	895±120	751±15	788±35	730±71
Ss 29	D	344	183	0.53	57	1831	0.1079(1.68)	0.1453(2.08)	2.1607(2.83)	0.0500(3.03)	1764±31	874±17	1169±20	986±29
Ss 30	D	392	172	0.44	39	1058	0.0571(4.47)	0.0930(2.08)	0.7320(5.16)	0.0280(4.93)	494±99	573±11	558±22	559±27
Ss 31	D	610	1150	1.89	94	1736	0.0583(2.56)	0.1066(2.07)	0.8567(3.49)	0.0325(2.24)	542±56	653±13	628±16	646±14

"Schistes Lustrés" of Piemont origin. The whole pile rests on top of the Gran Paradiso orthogneiss dome (Piemont Zone). The Cogne pre-Alpine intrusive, of calc-alkaline affinity (DESMONS and PLOQUIN, 1989; BONIN et al., 1993) was suspected to belong to the group of meta-igneous rocks now dated at ca. 500 Ma in the Briançonnais Zone. Two samples of metagranodiorites have been analysed (both sampled in a scree, downstream of the Cogne village). Sample ZH 95-19 is a light-coloured metagranodiorite containing quartz, albite, brown neo-biotite, remnants of a pale green amphibole, epidote and abundant titanite and zircon. Sample ZH 95-20 is a darker metagranodiorite in which amphibole is more abundant. Conventional U–Pb isotopic analyses were performed on zircons from sample ZH 95-20 and SHRIMP analyses on zircons from sample ZH 95-19. The zircon fractions prepared for the conventional study (ZH 95 20) are lilac colour and euhedral, but the surfaces of the zircon grains are often irregular with occasional smoothed edges. Only a few grains are easy to index using the PUPIN (1980) classification, and they suggest a calc-alkaline origin. BSEM images show a regular zoning of magmatic type, large apatite inclusions and irregular faces. The outer rim comprises a large number of tiny quartz inclusions (formed during overgrowth?). Zircons from sample ZH 95 19, analysed on SHRIMP II, have a very similar typology. BSEM images show a regular, magmatic zoning and suggest the presence of a recrystallised (nebulitic) core in some grains (Fig. 3).

Conventional analyses – Four out of five fractions from sample ZH 95-20 define an upper intercept age of 363 ± 24 Ma (MSWD = 0.13). All analytical points are highly discordant, and correspond to low $^{206}Pb/^{204}Pb$ ratios, even for the abraded fraction (B1), which explain the large errors in the age (Tab. 1 and Fig. 5a). One fraction (B0) is far from the discordia and suggests a Pan-African inheritance in the magma source.

SHRIMP results – Analytical results from sample ZH 95-19 (18 analyses on 16 zircon grains)

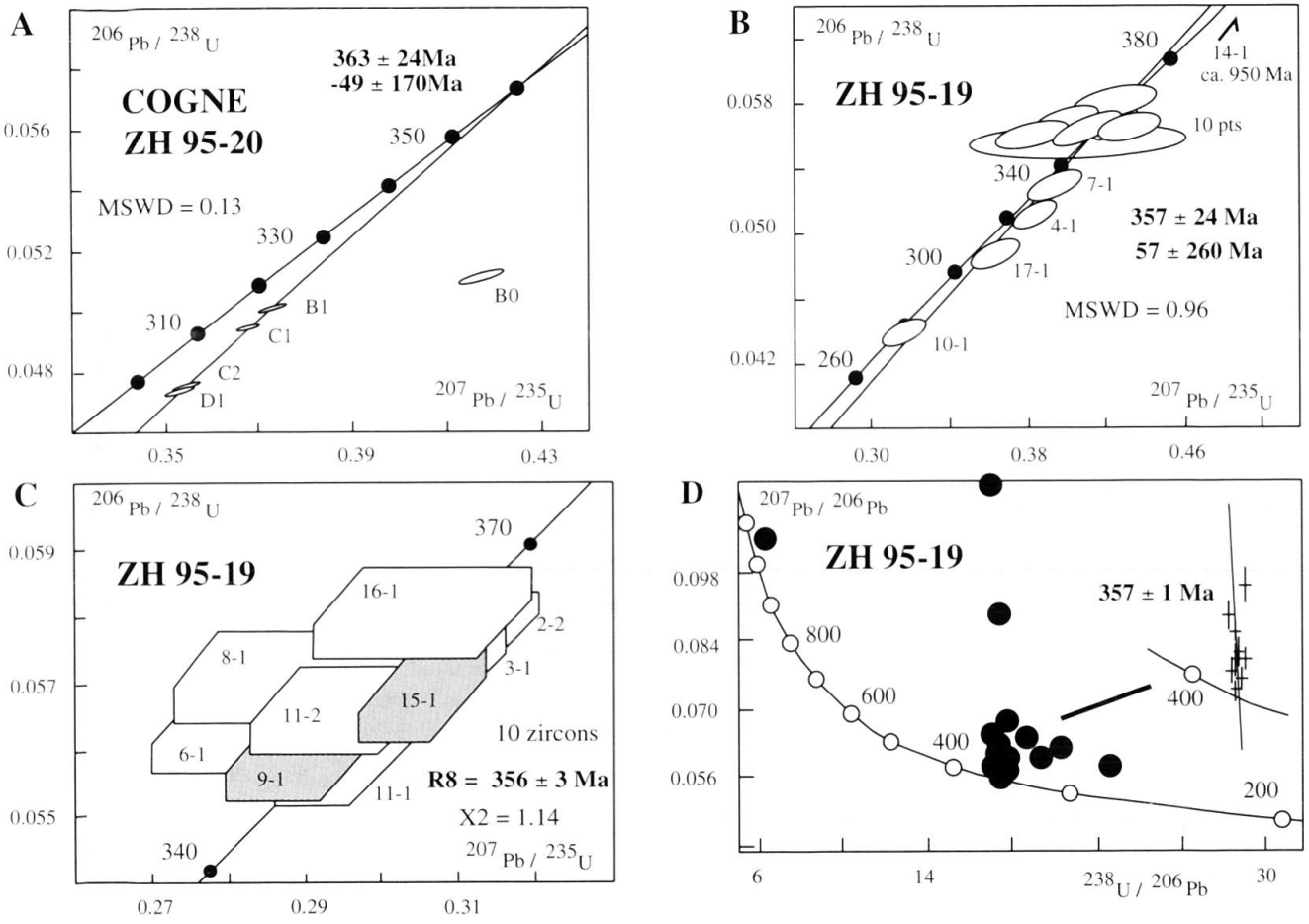

Fig. 5 Concordia diagram for Cogne granodiorites: (A) conventional data (sample ZH 95-20, 2σ errors); (B) SHRIMP data (sample ZH 95-19, 1σ errors) except inherited point at ca. 950 Ma; (C) enlargment of the 10 concordants points (filled boxes are cores); (D) Tera-Wasserburg diagram.

are given in table 2 and shown on figure 5. Data show high $^{206}Pb/^{204}Pb$ ratios except for three points which were not used for statistics. One analysis shows an inherited core at ca. 950 Ma (14-1). However, most data points are almost concordant and zoned domains or cores are not significantly different. Pooling together the 10 concordant points (Fig. 5c: 8 Z and 2 C) yields the following results: $^{206}Pb/^{238}U$ age = 356 ± 3 Ma (X^2 = 1.14); $^{207}Pb/^{235}U$ age = 356 ± 5 Ma (X^2 = 1.18); $^{207}Pb/^{206}Pb$ age = 352 ± 28 Ma (X^2 = 1.06). If zoned (Z) domains are treated separately (8 analyses) the results are very similar ($^{206}Pb/^{238}U$ age = 358 ± 4 Ma with X^2 = 0.72). Four analytical points yielded younger apparent ages. Two of the analyses have obviously suffered lead loss and two other spots (10-1, and 17-1) correspond to a small inclusion and a crack.

On the Tera-Wasserburg diagram (Fig. 5d) most of the points, except the four showing young apparent ages and the old core, are close to a lower intercept at 357 Ma.

4.3. THE AMBIN BASEMENT DOME

The Ambin massif outcrops as a large dome overlain by a parautochthonous Mesozoic Briançonnais-type cover and a thick pile of allochthonous "Schistes Lustrés" of oceanic Ligurian-Piemont origin (Fig. 1). The Ambin Formation forms the upper part of the basement dome (BORGHI and GATTIGLIO, 1997). It comprises high-pressure micaschists and conglomerates. Close to the geometrical top of the Ambin Formation, metarhyolites and greenstones occur on the Italian side. An underestimation of the tectonic nature of the contact between the Ambin Formation and overlying Permian and Triassic formations explains why, for a long time, the Ambin Formation was thought to be Permian in age.

Two samples have been analysed: 96 AM 4 (Casa Bolmi, Val Clarea) is a completely recrystallised metarhyolite with albitised and sericitised K-feldspar, fine-grained quartz and albite, phengite and secondary calcite and ankerite; 96 AM 6

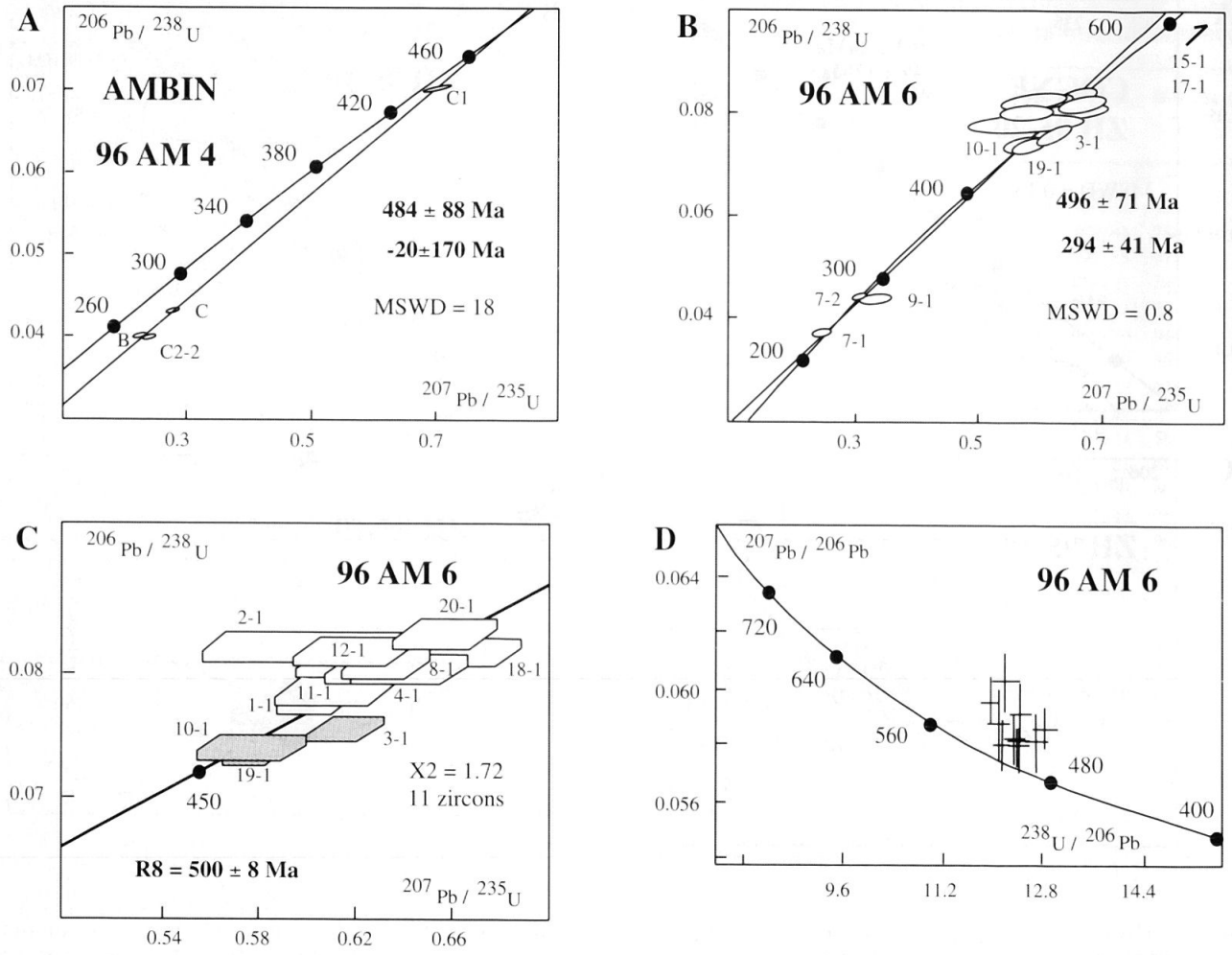

Fig. 6 Concordia diagram for Ambin metarhyolites: (A) conventional data (sample 96 AM 4, 2σ errors); (B) SHRIMP data (sample 96 AM 6, 1σ errors) except 2 inherited points at ca. 1835 and 2860 Ma; (C) enlargment of the 11 concordants points (filled boxes are cores); (D) Tera-Wasserburg diagram.

(Ramats, Valle d'Ulzio) is similar with more phengite, no calcite but some secondary hematite. In both samples zircons are very small (< 75 μm) and colourless except for some rare larger brown grains. The zircon crystals are of a poor quality for dating as they contain many tiny inclusions of quartz, biotite and xenotime. The typology is typically alkaline (PUPIN, 1980). BSEM images show faint or no zoning. The zircon population shows two contrasting grain types: small clear euhedral grains; and larger brown, euhedral grains, which are sometimes slightly rounded. The margin of several grains is outlined by a thin, lighter, discontinuous, outer zone which may correspond to tiny overgrowths and suggests a post-crystallisation event.

Conventional analyses – Six zircon fractions of the metarhyolite sample AM 96 4 were analysed using conventional techniques. Common lead levels were high, as indicated by low $^{206}Pb/^{204}Pb$ ratios especially for two fractions weighting less than 20 μg. This may be due to the numerous inclusions present in the zircon crystals (Tab. 1 and Fig. 6a). The four remaining points are poorly aligned and very discordant. They define an upper intercept at 484 ± 88 Ma (MSWD = 18) except for C1 ($^{207}Pb/^{206}Pb$ age of 487 ± 19 Ma). However, the average of the $^{207}Pb/^{206}Pb$ apparent ages for these four fractions yields an age of 496 ± 21 Ma which is considered as the best estimate for the crystallisation age.

SHRIMP results – Twenty-one analyses for 20 zircon grains from the metarhyolite sample 96 AM 6 are shown in table 2 and on figure 6. The $^{206}Pb/^{204}Pb$ ratios are high except for two points. Three groups may be defined from the Concordia diagram (Fig. 6b):

(1) Two zircon grains (15-1 and 17-1) correspond to $^{207}Pb/^{206}Pb$ ages of 1835 and 2860 Ma, respectively. One is rounded and the other is a polyfacetted brown grain.

(2) The main group, which is almost concordant, comprises 14 analyses corresponding to (H) type domains (Fig. 6c). Three analyses (19-1, 10-1 and 3-1) are located slightly below the main group; they are slightly discordant and may suggest lead loss. Pooling together the 11 remaining analyses, the obtained figures are: $^{206}Pb/^{238}U$ age = 500 ± 8 Ma (X^2 = 1.72); $^{207}Pb/^{235}U$ age = 494 ± 8 Ma (X^2 = 0.62); $^{207}Pb/^{206}Pb$ age = 478 ± 28 Ma (X^2 = 0.39). Zircons have a high Th content with a Th/U ratio between 0.5 and 1. The average $^{208}Pb/^{232}Th$ age for the whole group is 500 ± 15 Ma and is similar to the $^{206}Pb/^{238}U$ age.

(3) Three points (7-1, 7-2 and 9-1) are located far below the main group, between 240 and 280 Ma. The spot of grain 9-1 shows cracks and inclusions. Grain 7, where the two spots are located in a core zone, also shows micro-cracks. For these reason, they are not likely to correspond to a Permian event.

The Tera-Wasserburg diagram (Fig. 6d) shows that the points of the main group are not aligned, the scatter probably being the result of a combination of inheritance and lead loss.

4.4. THE GRAN PARADISO GNEISSIC DOME

The Gran Paradiso gneissic dome is the structurally deepest unit of the Piemont Zone. The gneisses are overlain by a thin metasedimentary cover, presumed to be Permian to Malm in age, and by the allochthonous "Schistes Lustrés", a high-pressure metamorphic assemblage of calcschists and metabasites derived from the Ligurian ocean. Two samples from the Ecot village have been analysed. A porphyritic orthogneiss (ZH 96 23) is the most common rock type in the whole massif, and its magmatic origin is well-established (BERTRAND, 1968; VEARNCOMBE, 1983). The rock contains large perthitic K-feldspars and biotite has been replaced by phengite, rutile and titanite with local crystallisation of neo-biotite and epidote. Rare chemical data suggest a sub-alkaline trend (BONIN et al., 1993). Another sample (ZH 96 24) is from a darker metre-size enclave in the orthogneiss; it comprises recrystallised K-feldspar, albite replacing an older plagioclase, large relict biotite, neo-biotite and secondary allanite. Both samples yielded euhedral zircons with numerous inclusions and obvious cores.

Zircon types observed in the orthogneiss (ZH 96-23) indicate a relatively high-temperature calc-alkaline typology (PUPIN, 1980). As shown from BSEM images, cores are obvious in many grains. They show a nebulitic recrystallisation pattern with white, irregular zones which may exist throughout the grain, and local concentrations of uranium-rich mineral inclusions (uranothorite, Fig. 3). Some grains are rounded and show an irregular recrystallisation of their margins forming "loops" of irregular and very thin zoning. However, some grains are perfectly euhedral and regularly zoned.

The dark enclave (sample ZH 96 24) has very similar zircon types. Cores have been identified in some grains. The zircon population is very heterogeneous in colour but most grains are euhedral. However, some are rounded and may correspond either to xenocrysts which have escaped any magmatic overgrowth or to scalped cores.

Conventional U–Pb isotopic analyses yielded poor alignments of the data points on a Concordia plot (data in table 1). Reference lines with high MSWD yield lower intercepts in the 198–204 Ma range and upper intercepts at ca. 1100–1200 Ma. The scattering of the analyses and the reverse discordia indicate a large inherited component suggesting that none of these ages has a geological significance.

SHRIMP results: the porphyritic orthogneiss – Twenty-four SHRIMP analyses were made on 23 zircon grains from the porphyritic orthogneiss (ZH 96-23) (Tab. 2 and Fig. 7a). Except for one point (24-1), the $^{206}Pb/^{204}Pb$ ratios are high. Four groups can be defined from the Concordia diagram (Fig. 7a):

(1) One old xenocryst (23-1), almost concordant at 1893 ± 4 Ma ($^{207}Pb/^{206}Pb$ age).

(2) Discordant analyses on indistinctly zoned domains and cores, spread between 350 and 650 Ma suggesting an upper intercept at ca. 640 Ma where two, almost concordant, points are located (9-1 and 11-1). The corresponding lower intercept is close to group (3).

(3) The main group of concordant points is centered at ca. 250–280 Ma (Fig. 7b). It comprises 2 cores located near the oldest end of the spread. Two other points are clearly separated from the main group at both ends (3-1 below and 5-1 above), both being slightly above the Concordia. The weighted mean of the 13 points (zoned domains and cores together) shows: $^{206}Pb/^{238}U$ age = 269 ± 6 Ma (X^2 = 2.33); $^{207}Pb/^{235}U$ age = 269 ± 6 Ma (X^2 = 1.33); $^{207}Pb/^{206}Pb$ age = 269 ± 19 Ma (X^2 = 0.63). For 11 points (deleting the two end points) the ages are identical except for better X^2 and a slightly older, but within an acceptable range of error, $^{207}Pb/^{206}Pb$ age = 274 ± 19 Ma (X^2 = 0.50).

(4) Two points located below the main group (3-1 and 20-1) probably correspond to lead loss.

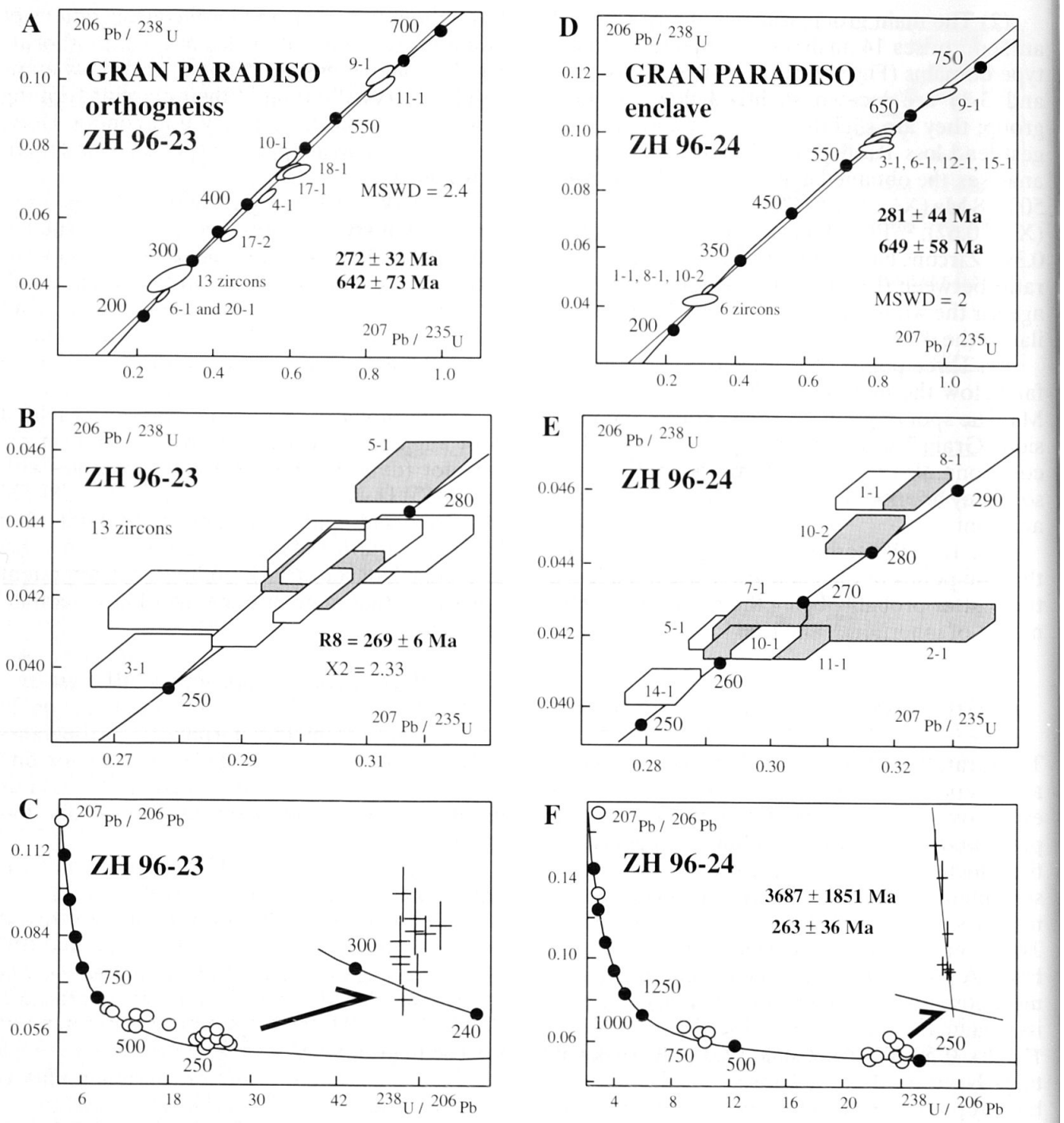

Fig. 7 Concordia diagram for Gran Paradiso orthogneiss (ZH 96-23) and dark enclave (ZH 96-24): (A) SHRIMP data (orthogneiss ZH 96-23, 1σ errors) except the 1893 Ma inherited zircon; (B) enlargment of the 11 concordants points (filled boxes are cores); (C) Tera-Wasserburg diagram for the orthogneiss sample; (D) SHRIMP data for the dark enclave, except the two inherited zircons at ca. 2000 and 2500 Ma; (E) enlargment of the ca. 270 Ma concordant points; (F) Tera-Wasserburg diagram for the enclave sample.

On the Tera-Wasserburg diagram (Fig. 7c), the 600 Ma group is scattered, having probably lost some lead. If we exclude the inherited grains of groups 1 and 2, the intercept at 271 Ma agrees with the above estimate.

SHRIMP results: the dark enclave – Analytical results from sample ZH 96-24 are given in table 2 (17 analyses out of 15 zircon grains). Except for one point, the $^{206}Pb/^{204}Pb$ ratios are all above 1000. Three groups may be defined from the location of the analytical points along the concordia (Fig. 7d). It is interesting to notice that 7 out of 17 analyses correspond to Precambrian ages. They are:

(1) Two old grains at ca. 2000 and 2500 Ma (7/6 ages) which clearly correspond to old xenocrysts.

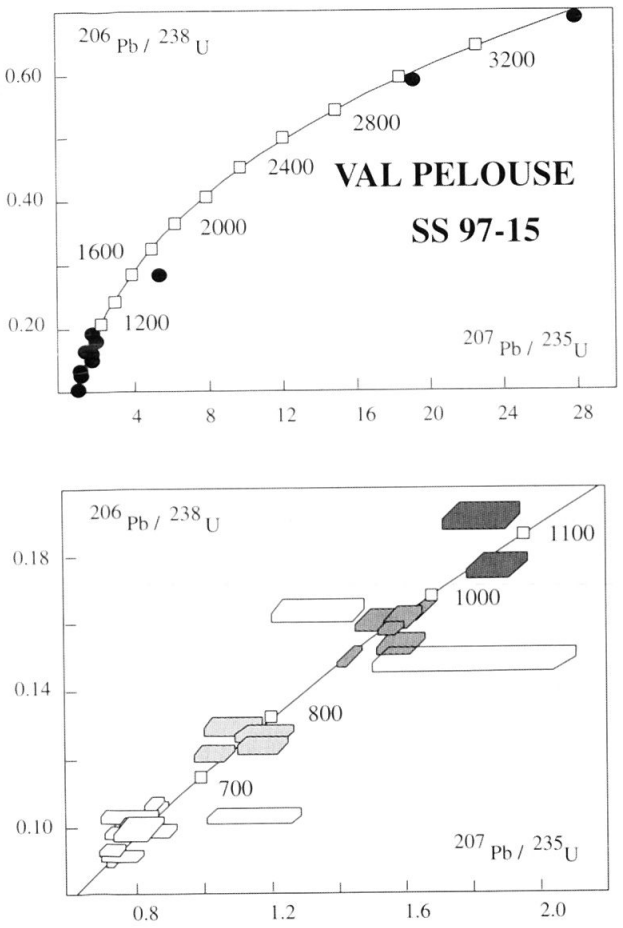

Fig. 8 SHRIMP concordia diagrams of the Val Pelouse detrital zircons.

(2) A well-defined group of four 600 Ma zircons (Fig. 7d) and one slightly older at 700 Ma, which are almost concordant. This suggests that they may correspond to a major event. The four points yield a weighted $^{206}Pb/^{238}U$ age of 597 ± 18 Ma ($X^2 = 2.08$).

(3) The 10 analytical points which constitute the "Variscan" group (Fig. 7e), are spread between 255 and 290 Ma. They are clearly separated into two sub-groups with one single point lying a little further below (the point with a low $^{206}Pb/^{204}Pb$ ratio has not been considered). $^{206}Pb/^{238}U$ ages are between 280 and 290 Ma for the older subgroup (3 points: 1-1, 8-1 and 10-2), but are located above the concordia, and between 260 and 270 Ma for the younger subgroup (5 points: 2-1, 5-1, 7-1, 10-1, 11-1). Point 14-1 is removed from the two subgroups and has a $^{206}Pb/^{238}U$ age of 257 Ma. The observed pattern is indeed ambiguous and the poorly statistically defined age of 270 Ma (only 5 points) is preferred because it is similar to the age defined by the orthogneiss (ZH 96-23). Examination of the Tera-Wasserburg diagram (Fig. 7f) favours this interpretation with a lower intercept at 263 ± 36 Ma.

4.5. THE "SÉRIE SATINÉE" OF BELLEDONNE

In contrast to the units described above, which belong to the Internal Domains, the "Série Satinée" belongs to the External Crystalline Massifs (ECM) and has been chosen as a comparison. The analysed sample belongs to an extensive mica-schist belt running along the western edge of the ECM. Our sample comes from a thin chloritic layer which has provided a small quantity of small, brown coloured, rounded zircons.

SHRIMP results – Thirty one zircon grains were analysed from sample SS 97 15 (Val Pelouse). Analytical spots were located near the centre of grains which are approximately 70 µm in diameter. There is no obvious correlation between the colour and shape of grains and their apparent ages. During this particular measurement session, abnormally high concentrations of common Pb were measured in both the analysed crystals and the standards. The reasons for this are unknown, but, together with the used analytical procedure (only four scans, see above), it leads to a greater degree of error in the results. Table 2 shows the analytical data for the 31 measurements. $^{207}Pb/^{206}Pb$ ages are preferred for Precambrian grains as recommended by CLAOUÉ-LONG et al. (1995). Four groups of data may be defined according to their location on the concordia (Fig. 8):

(1) Three old grains at ca. 2000, 3100 and 3400 Ma, the latter is one of the oldest zircon identified in European rocks (GEBAUER et al., 1989). One very discordant grain has a $^{207}Pb/^{206}Pb$ age of 1764 Ma. The analyses do not form an homogeneous group and may represent several detrital sources which may have been recycled a number of times as suggested by BSEM images which show complex patterns (Fig. 3).

(2) A distinct group of Grenvillian zircons with $^{207}Pb/^{206}Pb$ ages at about 800–1100 Ma is clearly seen. Discarding discordant points, the statistical pooling (4 points) yields a $^{207}Pb/^{206}Pb$ age of 975 ± 60 Ma ($X^2 = 2.36$). This almost concordant group suggests that a specific detrital source existed at that time.

(3) Four points are scattered around 750 Ma, but are discordant. It is not known if this group has a specific geological significance, as it is unknown elsewhere.

(4) Twelve zircons yielded a Pan-African age and form a homogeneous group on a concordia plot (Fig. 8). Averaging the data yields a $^{207}Pb/^{206}Pb$ age of 594 ± 36 Ma ($X^2 = 0.71$). This group of 12 zircon grains (more than a third of the total number of analyses) is almost concordant and

provides strong evidence for the prominence of a Pan-African source. However, 3 points which form the lowest part of the group are scattered and yield $^{207}Pb/^{206}Pb$ ages between 539 and 559 Ma. More data are needed to test whether these grains constitute a group of their own, which would provide a maximum age for the formation.

5. Discussion

5.1. BRIANÇONNAIS BASEMENT UNITS

Protolith zircons dated in the Briançonnais Zone are dominantly Cambrian to Ordovician in age. In the Sapey gneiss Unit (SGU) SHRIMP results from the Modane metagranite define a major event at 452 ± 5 Ma, and the Péclet orthogneiss has an older age of 482 ± 5 Ma. This older age is interpreted as the timing of zircon crystallisation in granitic protoliths. The age difference of 30 Ma between the Péclet orthogneiss and the Modane porphyritic metagranite suggests that several plutonic events occurred. The older Péclet orthogneiss (ZH 94-2) is heterogeneous and comprises numerous deformed aplitic and pegmatitic veins whilst the younger Modane metagranite (G94 004) is statically retrogressed and its granite texture is preserved. In both samples, Pan-African and less-marked ca. 1000 Ma inheritances were observed when dating xenocrystic cores, but even older inherited material is present. This explains why the conventional approach on multigrain fractions was unsuccessful and confirms that ion-probe in-situ isotope analysis is the best way to date polymetamorphic rocks.

In the Briançonnais basement, the Arpont metagranite was dated at 479 ± 6 Ma by the conventional method (BERTRAND and LETERRIER, 1997). This age corresponds to the emplacement age of an alkaline intrusive, but is slightly younger than other alkaline granite bodies in the Briançonnais basement dated at between 500 ± 2 Ma and 511 ± 9 Ma (GUILLOT et al., 1991; BUSSY et al., 1996; BERTRAND et al., 2000). The Arpont metagranite belongs to a bimodal volcano-plutonic association which is reminiscent of the "leptyno-amphibolite series" defined in the French Massif Central (see recent reviews in BARD, 1997; FAURE, 1996; FAURE et al., 1997). The lack of post-emplacement isotopic resetting suggests that the Variscan metamorphism was very weak in the Briançonnais basement.

The Ambin metarhyolites yielded similar ages for both conventional and SHRIMP techniques. SHRIMP results indicate a rather restricted Archean to Proterozoic inheritance (2 analyses on grain 21) and an age of 500 ± 8 Ma which is interpreted as the primary emplacement age of the rhyolites. There is no evidence of a Variscan event. The previously assumed Permian age of the Ambin Formation should therefore be dismissed. Such a Cambrian–Ordovician age questions the significance of the assumed older polymetamorphic Clarea Formation (BORGHI and GATTIGLIO, 1997) which forms the core of the Ambin alpine dome. Interestingly, the Early Paleozoic stratigraphic sequence defined in the low-grade formations of South Sardinia, outside of the Alpine belt, shows many similarities with the Ambin formation (references in CARMIGNANI et al., 1992). Taking this option a step further, the locally thick conglomerate layer that separates the Clarea Formation from the Ambin Formation could be considered as a remnant of an Early Paleozoic Gondwanian tillite. Consequently, other large metamorphic units, classically attributed to the Permian in the Briançonnais domain are probably of Early Paleozoic age.

In the Variscan belt of "stable Europe", Cambrian–Ordovician magmatic activity is related either to ophiolitic complexes – Chamrousse ophiolite (U–Pb age: PIN and CARME, 1987; MÉNOT et al., 1988) – or to a major extensional event described in many places in the Variscan belt, from Armorica, the southern French Massif Central, the Pyrenées through to Spain (references in PIN and MARINI, 1993; VALVERDE-VAQUERO and DUNNING, 2000). By contrast, numerous age data from the Central and Eastern Alps, especially in the Austro-Alpine and Southern Alpine domains suggest the existence of a major Ordovician orogenic event (reviews and discussions in: GEBAUER, 1993; VON RAUMER and NEUBAUER, 1993; NEUBAUER and VON RAUMER, 1993; VON RAUMER, 1998; SCHALTEGGER and GEBAUER, 1999). The open question now, is whether or not this Lower Paleozoic event, found in the "Intra-Alpine Terranes" (STAMPFLI, 1996), corresponds to extensional environments associated with pre-Variscan rifts or to remnants of an Ordovician orogenic belt clearly distinct from the Caledonian belt of northern Europe. Such an hypothesis is supported by the existence of eclogites and migmatites of Ordovician age (references in SCHALTEGGER and GEBAUER, 1999). From our recent data from the Western Alps, at least three age groups may be defined: ca. 510–500 Ma, ca. 480 Ma and ca. 450–460 Ma. Unfortunately both the geographical scatter of the analysed samples and the strong Alpine reworking hampers the establishment of a clear evolutionary scheme. Preliminary observations suggest two contrasting geochemical affinities and time relationships: alkaline for Mont

Pourri (GUILLOT et al., 1991), Finestre (BERTRAND et al., 2000), Arpont (BERTRAND and LETERRIER, 1997), Ambin (this study) and Thyon (BUSSY et al., 1995)) in the ca. 510–500 Ma age range (except for Arpont); and calc-alkaline for the 480–450 Ma Sapey gneisses. If the 496 Ma Chamrousse ophiolite from the ECM (MÉNOT et al, 1988 b) is taken as a fixed time-reference – neglecting the fact that it belongs to the foreland (External Alps) – the hypothetical Ordovician orogenic cycle was short-lived between ca. 510–480 Ma (extension, rifting, local oceanic crust), to ca. 480–460 Ma (deformation and metamorphism: collision?) and finally ca. 450 Ma (late-orogenic plutonism and/or anatexis?). As for the Visean event described in the ECM, the Vosges and the Black Forest massifs (SCHALTEGGER and CORFU, 1995; SCHALTEGGER et al., 1996; SCHALTEGGER et al., 1999; SCHALTEGGER, 2000) or for the Permian event (VON RAUMER and NEUBAUER, 1993), a Basin and Range-type environment (SCHALTEGGER and CORFU, 1995) is an interesting alternative, some areas having enjoyed a complete orogenic cycle while other areas show only extensional magmatism, albeit not far from an active margin which helps to explain the coexistence of alkaline and calc-alkaline magmas. In this case, the observed mixture of ages and geochemical affinities could result, not only from an exotic terrane origin for the Penninic domain with respect to the ECM, but also, as suggested by GIORGIS et al. (1999), from the fact that the Penninic domain itself corresponds to a collage of several contrasting Paleozoic terranes.

Contrasting with these old ages, the 356 Ma Cogne plutonic body appears to be the only evidence for Variscan magmatic activity in the Briançonnais Zone. It is older than previously measured metamorphic ages in a neighbouring tectonic unit (BUSSY et al., 1996; GIORGIS et al., 1999) and older than the 324 Ma Costa Citrin granite in the ZHB (BERTRAND et al., 1998). SHRIMP data indicate that, except for a restricted lead loss and the recognition of a single xenocrystic core (ca. 950 Ma old), zircons from sample ZH 95 19 belong to a single population which crystallised during the emplacement of the Cogne granodiorite 356 ± 3 Ma ago. Conventional data yield a similar but less precise age. No evidence has been found of a late Variscan imprint. As ages in this range are scarce in the Variscan belt (e.g. MÉNOT et al., 1988b), it is now necessary to study in detail the units surrounding this large intrusive body to determine its pre-Alpine significance. If compared with other parts of the Variscan belt, the Cogne intrusion could represent a remnant of an early magmatic arc (subduction-related? – what subduction?).

5.2. PIEMONT BASEMENT UNITS

Interpretation of deep seismic data suggests that the Piemont Zone may be considered as the subducted passive margin of the European plate (SCHMID et al., 1996; SCHMID and KISSLING, 2000) but, it may also correspond to high-pressure metamorphosed slices of the Apulian plate (STAMPFLI et al., 1998). Only the Dora Maira massif has been confidently dated (BUSSY and CADOPPI, 1996): an Ordovician augengneiss (Punta Muret, ultra-high-pressure) at 457 ± 2 Ma; late Carboniferous intrusives (Malanaggio diorite at 290 ±2 Ma and Cavour leucogranite at 304 ± 2 Ma) and Permian intrusives (Sangone granite at 267–279 Ma and Freidour granite at 268–283 Ma).

The Gran Paradiso metagranite, previously believed to be Carboniferous, yielded a Permian age. SHRIMP analyses have shown that the lower intercept ages yielded by conventional analyses (ca. 200 Ma), reminiscent to the lower intercept age yielded by zircons of the Monte Rosa orthogneiss (PAQUETTE et al., 1989), are not geologically significant. They result from lead loss, together with a complex inheritance pattern, which comprises of, at least two main inherited sources at ca. 2000–2500 Ma and ca. 600–700 Ma. Although the morphology of most of the zircons is obviously magmatic, the age pattern of the dark enclave sample (ZH 96 24) suggests a detrital population which may derive from a raft of partly melted country rock. The statistically best defined age of 269 ± 6 Ma, based upon the analyses of the zircon tips from the orthogneiss sample (ZH 96-23), is interpreted as the emplacement age of the Gran Paradiso granitic protolith.

Such Permian ages are definitely younger than the latest stages, dated at ca. 300–290 Ma, of the Variscan orogeny as described in the ECM (Mont Blanc and Aar massifs: BUSSY and VON RAUMER, 1994; SCHALTEGGER, 1994). Intrusives of Permian age are known in the Briançonnais and Piemont nappes (Randa orthogneiss, BUSSY et al., 1996; Truzzo and Roffna granitoids, MARQUER et al., 1998; a monazite age in Monte Rosa, KÖPPEL and GRÜNENFELDER, 1975; Dora Maira, BUSSY and CADOPPI, 1996; Fedoz gabbro, HERMANN et al., 1997). Similar ages are also quoted from recent studies in the Ivrea zone and in the Austro-Alpine domain (see review in SCHALTEGGER and GEBAUER, 1999). Together with the abundance of Permian volcanics, these results point to the occurrence of a major (extensional?) Permian event in the Internal Alps. They suggest that the Piemont basement massifs and perhaps part of the Briançonnais Zone (MARQUER et al., 1998) may have been derived from a specific segment of the Variscan

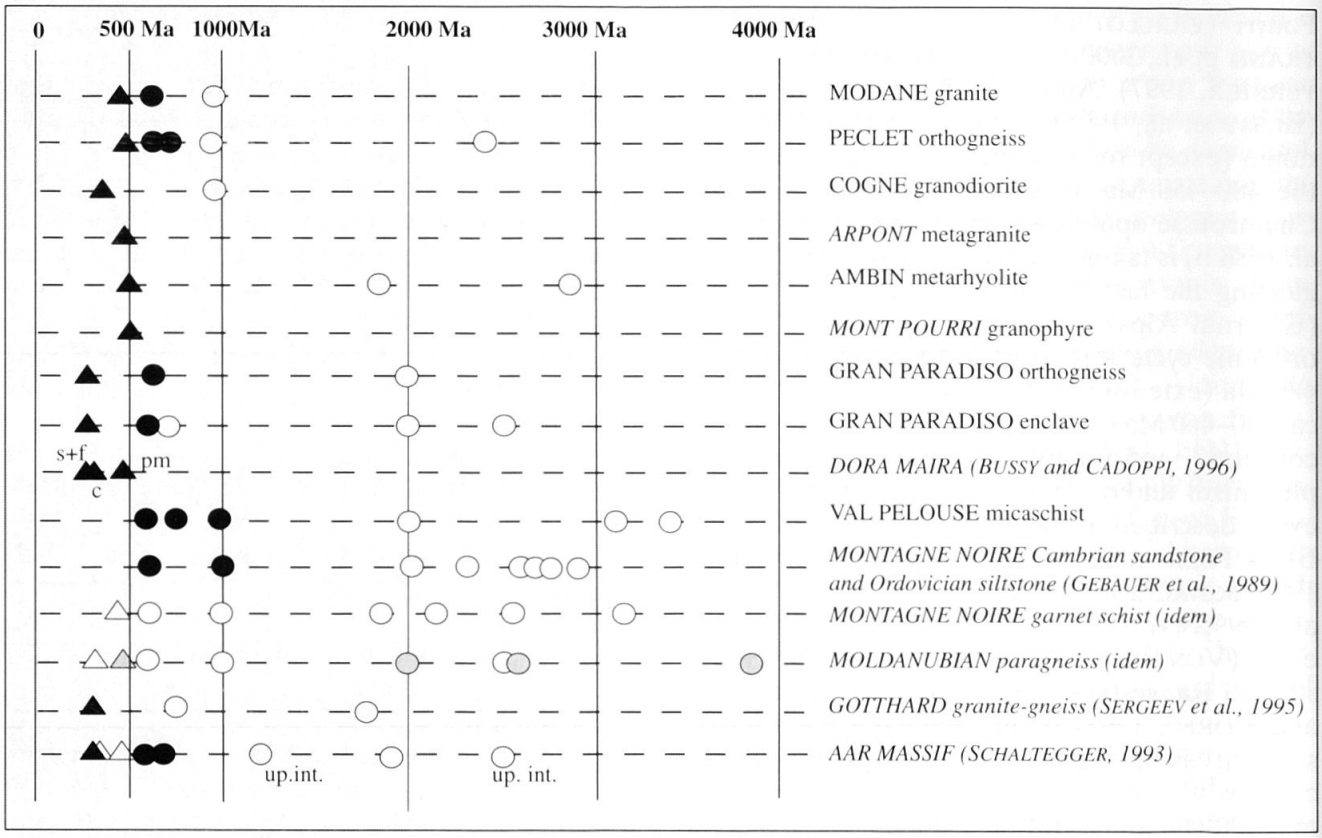

Fig. 9 Comparison of magmatic, metamorphic, detrital and xenocrystic ages. Reference data are in italics. Circles correspond to xenocrysts or detrital zircons (empty circles: 7/6 ages for one concordant zircon; filled circle: 7/6 ages for several grains). Triangles are metamorphic (empty) and magmatic (filled) zircons – grey triangle and circles correspond to GEBAUER et al. (1989) measurements of successive growth of the same zircon grain.

belt or from a post-Variscan, early Tethyan orogenic belt.

5.3. DETRITAL ZIRCONS FROM THE EXTERNAL CRYSTALLINE MASSIFS

The "Série Satinée" of the Belledonne massif was selected as a suitable reference for a pre-Variscan sedimentary representative of pre-Alpine "stable" Europe. Preliminary results showed that the "Serie Satinée" is post Pan-African in age as detrital zircons originating from a Pan African source are the most common. The youngest detrital zircons, dated at 594 Ma, suggest a Cambrian maximum age for the deposition of the analysed rock. Other inherited ages (3400, 3100, 2000, 1000 Ma) are very similar to the age spectra determined in the Montagne Noire region and in the Moldanubian domain (GEBAUER et al., 1989). If age spectra are compared, xenocrystic zircons from the SGU and Gran Paradiso and detrital zircons of the "Série Satinée" are also very similar. This suggests that at crustal scale, the difference between the External domain and the Briançonnais domain may be small. A comparison of detrital ages from the literature (GEBAUER, 1993; SCHALTEGGER, 1994; SCHALTEGGER and GEBAUER, 1999; SERGEEV et al., 1995) with ages obtained for cores and/or xenocrystic zircons from our samples showed that a Pan-African source is conspicuous in most of the analysed samples (Fig. 9). Pan-African ages (ca. 600 Ma) represent an unambiguous signature for the Precambrian Gondwana and confirm that all the pre-Alpine crust reworked within the Alpine belt was part of Gondwana-derived segments of the Variscan belt.

6. Conclusions

Our studies in the Briançonnais Zone of the Western Alps generally yielded ages within the 450–500 Ma range, which are significantly older than the previously assumed Variscan ages. The Cogne plutonic body and the Costa Citrin are the only Variscan intrusives identified so far. Thus the Briançonnais basement does not show the intense plutonic activity that occurred between ca. 335 Ma and ca. 300 Ma in the External Crystalline Massifs of the Western Alps (BUSSY et al., 1989; BUSSY and VON RAUMER, 1994; DEBON et al., 1998;

DEBON and LEMMET, 1999). This difference supports an exotic origin for the Briançonnais terrane, which has been suggested by some authors (STAMPFLI, 1993; RICOU, 1980), to be connected to Spain or Corsica-Sardinia and to have reached its present position either during the Variscan assembly of Gondwanian terranes, or during sinistral displacements of rifted blocks along the European margin during the early stages of the Alpine evolution. This implies large lateral displacements (RICOU, 1980) which may explain the strong stratigraphical contrast between the External Helvetic domain and the Briançonnais Zone. Such displacements may also have been initiated during the Carboniferous (significance of the ZHB basin?) and could explain the possible Permian event observed in the Piemont Zone and in the easternmost Briançonnais units in Switzerland (MARQUER et al., 1998).

If the Briançonnais Zone is compared with "stable" Variscan Europe and with the allochthonous Austro-Alpine/South Alpine domains, the following similarities and singularities may be outlined:

– A similar Pan-African inheritance has been demonstrated.

– A major Lower Paleozoic event is prominent in the Briançonnais and similar ages have been quoted in the Variscan belt, although the significance of the event has still to be determined in each domain.

– The scarcity of Variscan ages in the basement units.

The Permian ages yielded by metagranites of the Piemont Zone may imply that several allochthonous terranes constitute the Internal Alps East of the Penninic Front. This provides a new question: are they Variscan or Alpine terranes? The late-Variscan paleogeography was probably oblique to the site of the Alpine arc-shaped belt, including probably a 90° rotation of Sardinia as suggested by VAI and COCOZZA (1986). However, there is no clear data to distinguish between (i) the result of a large (and polyphased?) Alpine shortening which telescoped distinct domains of the Variscan crust during the Alpine collision and/or exhumation stages, (ii) large-scale lateral displacement and/or rotations of rifted blocks (the Permian event?) and (iii) the result of a possible Paleo-Tethys subduction (FINGER and STEYRER, 1990; ZIEGLER, 1993). Ages and metamorphic data obtained for the pre-Alpine terranes should only be used with caution when rebuilding the Late Permian to Triassic plate puzzle. The sharp break, usually assumed between Africa-derived domains and Variscan Europe, is probably a myth, seeing as both basement units comprise of, ultimately, Gondwanian material with traces of a Variscan activity.

Acknowledgements

This study was funded by CNRS (Centre de Recherches Pétrographiques et Géochimiques, Nancy, and Laboratoire de Géodynamique des Chaînes Alpines, Chambéry), by the GéoFrance3D project (CNRS-INSU, BRGM and MENRT) and by the French Embassy in Canberra. Thanks to Urs Schaltegger who accepted to criticise an early version of the paper and to the "Parc de la Vanoise" who authorised to sample in a protected area. Constructive reviews by F. Bussy and J.J. Peucat were also greatly appreciated. C. Hetherington polished the English. GéoFrance3D contribution N° 99.

References

AILLÈRES, L., BERTRAND, J.M., MACAUDIÈRE, J. and CHAMPENOIS, M. (1995): Structure de la Zone Houillère Briançonnaise (Alpes françaises), tectonique néoalpine et conséquences sur l'interprétation des Zones Penniques Frontales. C. R. Acad. Sci. Paris, II, 321, 247–254.

AMSTUTZ, A. (1962): Notice pour une carte géologique de la vallée de Cogne et de quelques autres espaces au sud d'Aoste. Arch. Sci., Genève, 15, 1–104.

BARD, J.P. (1997): Démembrement anté-mésozoïque de la chaîne varisque d'Europe occidentale et d'Afrique du Nord: rôle essentiel des grands décrochements transpressifs dextres accompagnant la rotation-translation horaire de l'Afrique durant le Stéphanien. C. R. Acad. Sci. Paris, II, 324, 693–704.

BEARTH, P. (1952): Geologie und Petrographie der Monte Rosa. Beitr. geol. Karte Schweiz, NF 96, 94 pp.

BERTRAND, J.M. (1968): Etude structurale du versant occidental du massif du Grand Paradis (Alpes Graies). Trav. Lab Géol. Grenoble, 44, 55–87.

BERTRAND, J.M., AILLÈRES, L., GASQUET, D. and MACAUDIÈRE, J. (1996): The Pennine Front zone in Savoie (western Alps), a review and new interpretations. Eclogae geol. Helv., 89, 297–320.

BERTRAND, J.M. and LETERRIER, J. (1997): Granitoïdes d'âge paléozoïque inférieur dans le socle de Vanoise méridionale: géochronologie U–Pb du métagranite de l'Arpont (Alpes de Savoie, France). C. R. Acad. Sci. Paris, Earth Planet. Sci., 325, 839–844.

BERTRAND, J.M., GUILLOT, F., LETERRIER, J., PERRUCHOT, M.P., AILLÈRES, L. and MACAUDIÈRE, J. (1998): Granitoïdes de la zone houillère briançonnaise en Savoie et en Val d'Aoste (Alpes occidentales): géologie et géochronologie U–Pb sur zircon. Geodin. Acta, 11, 33–49.

BERTRAND, J.M., GUILLOT, F. and LETERRIER, J. (2000): Age Paléozoïque inférieur (U–Pb sur zircon) de métagranophyres de la nappe du Grand-Saint-Bernard (zona interna, vallée d'Aoste, Italie). C. R. Acad. Sci. Paris, Earth Planet. Sci., 330, 473–478.

BONIN, B., BRÄNDLEIN, P., BUSSY, F., DESMONS, J., EGGENBERGER, U., FINGER, F., GRAF, K., MARRO, C., MERCOLLI, I., OBERHÄNSLI, R., PLOQUIN, A., VON QUADT, A., VON RAUMER, J., SCHALTEGGER, U., STEYRER, H.P., VISONÀ, D. and VIVIER, G. (1993): Late Variscan Magmatic evolution in the Alpine basement. In: VON RAUMER, J. and NEUBAUER, F.

(eds): Pre-Mesozoic Geology in the Alps. Springer-Verlag, Berlin, 171–201.

BORGHI, A. and GATTIGLIO, M. (1997)): Osservazioni geologico-petrografiche nel settore meridionale del massicio d'Ambin. Atti Tic. Sci. Terra, 5, 64–84.

BORGHI, A., COMPAGNONI, R. and SANDRONE R. (1994): Evoluzione termo-tettonica alpina del settore settentrionale del massicio del Gran Paradiso (Alpi Occidentali). Atti Tic. Sci. Terra (Serie speciale) 1, 137–152.

BUSSY, F. and VON RAUMER, J.F. (1994): U–Pb geochronology of Palaeozoic magmatic events in the Mont-Blanc Crystalline Massif, Western Alps. Schweiz. Mineral. Petrogr. Mitt., 74, 514–515.

BUSSY, F. and CADOPPI, P. (1996): U–Pb zircon dating of granitoids from the Dora Maira massif (western Italian Alps). Schweiz. Mineral. Petrogr. Mitt., 76, 217–233.

BUSSY, F., DERRON, M.H., JACQUOD, J., SARTORI, M. and THÉLIN, P. (1995): The 500 Ma-old Thyon metagranite : a new A-type granite occurrence in the Penninic realm (Western Alps, Wallis, Switzerland). Eur. J. Mineral., 8, 565–575.

BUSSY F., SARTORI. M. and THÉLIN P. (1996): U–Pb zircon dating in the middle Penninic basement of the Western Alps (Valais, Switzerland. Schweiz. Mineral. Petrogr. Mitt., 76, 81–84.

BUSSY, F., SCHALTEGGER, U. and MARRO, C. (1989): The age of the Mont Blanc granite (western Alps): a heterogeneous isotopic system dated by Rb–Sr whole rock determinations on its microgranular enclaves. Schweiz. Mineral. Petrogr. Mitt., 69, 3–13.

CABY, R. (1996): Low-angle extrusion of high-pressure rocks and the balance between outward and inward displacements of Middle Penninic units in the western Alps. Eclogae geol. Helv., 89, 229–267.

CARMIGNANI, L., BARCA, S., CAPELLI, B., DIPISA, A., GATTIGLIO, M., OGGIANO, G. and PERTUSATI, P.C. (1992): A tentative geodynamic model for the Hercynian basement of Sardinia. In: CARMIGNANI, L. and SASSI, F.P. (eds): Contributions to the Geology of Italy with special regard to the Paleozoic basement. IGCP N° 276, Newsletter Vol. 5, Siena, 61–82.

CHOPIN, C. and MALUSKI, H. (1980): ^{40}Ar–^{39}Ar dating of high-pressure metamorphic micas from the Gran Paradiso area (Western Alps): evidence against the blocking temperature concept. Contrib. Mineral. Petrol., 74, 391–394.

CLAOUÉ-LONG, J.C., COMPSTON, W., ROBERTS, J. and FANNING, C.M. (1995): Two carboniferous ages: a comparison of SHRIMP zircon dating with conventional zircon ages and $^{40}Ar/^{39}Ar$ analysis. In: Geochronology Time Scale and Global Stratigraphic Correlation, SEPM (Society for Sedimentary Geology), Spec. Publ. 54, 3–21.

COMPSTON, W., WILLIAMS, I.S. and MEYER, C. (1984): U–Pb geochronology of zircons from lunar breccia 73217 using a sensitive high mass-resolution ion microprobe. J. Geophys. Res., 89 (supl.), B 525–534.

CORTESOGNO L., DE STEFANO, L., GAGGERO, L. and SENO, S. (1996): Granodiorites in the Ligurian Briançonnais volcano-sedimentary Permian sequences: structural and petrochemical characterization. Atti Tic. Sci. Terra, (Serie speciale), 4, 87–101.

DEBELMAS, J. and LEMOINE, M. (1970): The Western Alps: paleogeography and structure. Earth Sci. Reviews, 6, 221–256.

DEBON, F., GUERROT, C., MÉNOT, R.P, VIVIER, G. and COCHERIE, A. (1998): Late Variscan granites of the Belledonne massif (French Western Alps): an Early Visean magnesian plutonism. Schweiz. Mineral. Petrogr. Mitt., 78, 67–85.

DEBON, F. and LEMMET, M. (1999): Evolution of Mg/Fe ratios in Late Variscan plutonic rocks from the External Crystalline Massifs of the Alps (France, Italy, Switzerland). J. Petrol., 40, 1151–1185.

DESMONS, J. and PLOQUIN, A. (1989): Géochimie du Briançonnais-Grand Saint Bernard antémésozoïque (Alpes occidentales). Géol. Alpine, 65, 1–31.

DESMONS, J., COMPAGNONI, R., CORTESOGNO, L., FREY, M. and GAGGERO, L. (1999): Pre-Alpine metamorphism of the Internal zones of the Western Alps. Schweiz. Mineral. Petrogr. Mitt., 79, 23–39.

DÉTRAZ, G. (1984): Etude géologique du bord interne de la zone Houillère briançonnaise entre la vallée de l'Arc et le massif de Péclet-Polset (Alpes de Savoie). Thèse Univ. Grenoble, 159 pp. et annexes.

ELLENBERGER, F. (1958): Etude géologique du Pays de Vanoise. Mém. Carte Géol. France, 561 pp.

FAURE, M. (1996): Late orogenic carboniferous extensions in the Variscan French Massif Central. Tectonics, 14, 132–153.

FAURE, M., LELOIX, C. and ROIG, J.Y. (1997): L'évolution polycyclique de la chaîne hercynienne. Bull. Soc. Géol. France, 168, 695–705.

FINGER, F. and STEYRER, H.P. (1990): I-type granitoids as indicators of a late Paleozoic convergent ocean-continent margin along the southern flank of the central European Variscan orogen. Geology, 18, 1207–1210.

FUDRAL, S. (1998): Etude géologique de la suture téthysienne dans les Alpes Franco-italiennes de la Doire Ripaire (Italie) à la région de Bourg-Saint-Maurice (France). Géol. Alpine, Mém. Hors série N° 29, 306 pp.

FREEMAN, S.R., INGER, S., BUTLER, R.W.H. and CLIFF, R.A. (1997): Dating deformation using Rb–Sr in white micas: Greenschist facies deformation ages from the Entrelor shear zone, Italian Alps. Tectonics, 16, 57–76.

FÜGENSCHUH, B., LOPRIENO, A., CERIANI, S. and SCHMID, S.M. (1999): Structural analysis of the Subbriançonnais and Valais units in the area of Moûtiers (Savoy, Western Alps) : paleogeographical and tectonic consequences. Int. J. Earth Sci., 88, 201–218.

GANNE, J. (1999): Evolution tectono-métamorphique de la partie NW du massif d'Ambin (Alpes penniques nord-occidentales, Savoie). Diplôme Études Approfondies, Univ. Savoie, Chambéry.

GEBAUER, D. (1993): The pre-Alpine evolution of the continental crust of the Central Alps – an overview. In: VON RAUMER, J. and NEUBAUER, F. (eds): Pre-Mesozoic Geology in the Alps. Springer-Verlag, Berlin, 93–117.

GEBAUER, D. and RUBATTO, D. (1998): 35 Ma-old UHP-metamorphism of the Dora Maira massif and other Tertiary HP- and UHP events in the Central and Western Alps: geodynamic consequences. Schweiz. Mineral. Petrogr. Mitt., 78, 199–200.

GEBAUER, D., WILLIAMS, I.A., COMPSTON, W. and GRÜNENFELDER, M. (1989): The development of the Central European continental crust since the Early Archaean based on conventional and ion-microprobe dating of up to 3.84 b.y. old detrital zircons. Tectonophysics, 157, 81–96.

GIORGIS, D., THÉLIN, P., STAMPFLI, G. and BUSSY, F. (1999): The Mont-Mort metapelites: Variscan metamorphism and geodynamic context (Briançonnais basement, Western Alps, Switzerland). Schweiz. Mineral. Petrogr. Mitt., 79, 381–398.

GUILLOT, F., LIÉGEOIS, J.P. and FABRE, J. (1991): Des granophyres du Cambrien terminal dans le Mont Pourri (Vanoise, zone briançonnaise): première datation U–Pb sur zircon d'un socle des zones internes

des Alpes françaises. C. R. Acad. Sci. Paris, II, 313, 239–244.

GUILLOT, F., DESMONS, J. and PLOQUIN, A. (1993): Lithostratigraphy and geochemical composition of the Mt. Pourri volcanic basement, Middle Penninic W-Alpine zone, France. Schweiz. Mineral. Petrogr. Mitt., 73, 319–334.

GUILLOT, F., BERTRAND, J.M., SCHALTEGGER, U. and LETERRIER, J. (2000) : Complémentarité entre dilution isotopique et sonde ionique: datation U–Pb de socles polycycliques alpins. 18éme R.S.T., Paris, résumés p. 151.

HERMANN, J., MÜNTENER, O., TROMMSDORFF, V., HANSMANN, W. and PICARDO, G.B. (1997): Fossil crust-to-mantle transition, Val Malenco (Italian Alps). J. Geophys. Res., B102, 20123–20132.

HUNZIKER, J.C., DESMONS, J. and HURFORD, A.J. (1992): Thirty-two years of geochronological work in the Central and Western Alps: a review on seven maps. Mém. Géol. Lausanne ,13, 1–59.

KÖPPEL, V. and GRÜNENFELDER, M. (1975): Concordant U–Pb ages of monazite and xenotime from the Central Alps and the timing of high temperature Alpine metamorphism: a preliminary report. Schweiz. Mineral. Petrogr. Mitt., 55, 129–132.

KROGH, T.E. (1973): A low-contamination method for hydrothermal decomposition of zircon and extraction of U and Pb for isotopic age determination. Geochim. Cosmochim. Acta, 37, 485–494.

LUDWIG, K.R. (1999): User's manual for Isoplot/Ex version 2. 10. Berkeley Geochronology Center, Spec. Publ., 1a, 49 pp.

MARQUER D., CHALLANDES, N. and SCHALTEGGER, U. (1998): Early Permian magmatism in Briançonnais terranes: Truzzo granite and Roffna rhyolite (eastern Penninic nappes, Swiss and Italian Alps). Schweiz. Mineral. Petrogr. Mitt., 78, 397–414.

MÉNOT, R.P., PEUCAT, J.J. and PAQUETTE, J.L. (1988a) : Les associations magmatiques acide-basique paléozoïques et les complexes leptyno-amphiboliques: les corrélations hasardeuses. Exemples du massif de Belledonne (Alpes occidentales). Bull. Soc. Géol. France, 8, IV, 917–926.

MÉNOT, R.P., PEUCAT, J.J., SCARENZI, D. and PIBOULE, M. (1988b): 496 Ma age of plagiogranites in the Chamrousse ophiolite complex (external crystalline massifs in the French Alps): evidence of a Lower Paleozoic oceanization. Earth Planet. Sci. Lett., 39, 98–708.

MONIÉ, P. (1990): Preservation of Hercynian $^{40}Ar/^{39}Ar$ ages through high-presure low-temperature alpine metamorphism in the western Alps. Eur. J. Mineral., 2, 343–361.

MUGNIER, J.L., LOUBAT, H. and CANNIC, S. (1993): Correlation of seismic images and geology at the boundary between Internal and External domains of the Western Alps. Bull. Soc. Géol. France, 164, 697–708.

NELSON, D.R. (1997): Compilation of SHRIMP U–Pb zircon chronology data, 1996. Geol. Surv. Western Australia, Department of Minerals and Energy. Record 1997/2.

NEUBAUER, F. and VON RAUMER, J.F. (1993): The Alpine basement – linkage between Variscides and East-Mediterranean mountain belts. In: VON RAUMER, J. and NEUBAUER, F. (eds): Pre-Mesozoic Geology in the Alps. Springer-Verlag, Berlin, 641–663.

PAQUETTE , J.L., CHOPIN, C. and PEUCAT, J. (1989): U–Pb zircon, Rb–Sr and Sm–Nd geochronology of high- to very-high-pressure meta-acidic rocks from the western Alps. Contrib. Mineral. Petrol., 101, 280–289.

PARRISH, R.R. (1987): An improved micro-capsule for zircon dissolution in U–Pb geochronology. Chem. Geol., 66, 99–102.

PIDGEON, R.T., FURFARO, D., KENNEDY, A.K., NEMCCHIN, A.A. and VAN BROSWJK, W. (1994): Calibration of zircon standard for the Curtin SHRIMP II. 8th Intern. Conf. on Geochronology, Cosmochronology and Isotope Geology, US Geological Survey Circular 1107, Abstracts, Berkeley, California, p. 251.

PIN, C. and CARME, F. (1987): A Sm–Nd isotopic study of 500 Ma old oceanic crust in the Variscan belt of western Europe: the Chamrousse ophiolite complex, western Alps (France). Contrib. Mineral. Petrol., 96, 406–413.

PIN, C. and MARINI, F. (1993): Early Ordovician continental break-up in Variscan Europe: Nd–Sr isotope and trace element evidence for bimodal igneous associations of the Southern Massif Central, France. Lithos, 29, 177–196.

PUPIN, J.P. (1980): Zircon and granite petrology. Contrib. Mineral. Petrol., 73, 207–220.

RICOU, L.E. (1980): La zone sub-briançonnaise des Alpes occidentales interprétée comme la trace d'un ample décrochement senestre sub-méridien. C. R. Acad. Sci. Paris, II, 290, 835–838.

RICOU, L.E. and SIDDANS, A.W.B. (1986): Collision tectonics in the Western Alps. In: COWARD, M.P. and RIES, A.C. (eds): Collision Tectonics. Geol. Soc. London, Spec. Publ., 19, 229–244.

SCHALTEGGER, U. (1993): The evolution of the polymetamorphic basement in the Central Alps unravelled by precise U–Pb zircon dating. Contrib. Mineral. Petrol., 113, 466–478.

SCHALTEGGER, U. (1994): Unravelling the pre-Mesozoic history of Aar and Gotthard massifs (Central Alps, Switzerland) by isotopic dating – a review. Schweiz. Mineral. Petrogr. Mitt., 74, 41–51.

SCHALTEGGER, U. (2000): U–Pb geochronology of the Southern Black Forest batholith (Central Variscan Belt): timing of exhumation and granite emplacement. Int. J. Earth Sci., 88, 814–828.

SCHALTEGGER, U. and CORFU, F. (1995): Late Variscan "Basin and Range" magmatism and tectonics in the Central Alp: evidence from U–Pb geochronology. Geodin. Acta, 8, 82–98.

SCHALTEGGER, U., SCHNEIDER, J.L., MAURIN, J.C. and CORFU, F. (1996): Precise U–Pb chronometry of 345–340 Ma old magmatism related to syn-convergence extension in the southern Vosges (Central Variscan Belt). Earth Planet. Sci. Lett., 144, 403–419.

SCHALTEGGER, U. and GEBAUER, D. (1999): Pre-Alpine geochronology of Central, Western and Southern Alps. Schweiz. Mineral. Petrogr. Mitt., 79, 79–87.

SCHALTEGGER, U., FANNING, C.M., GÜNTHER, D., MAURIN, J.C., SCHULMANN, K. and GEBAUER, D. (1999): Growth, annealing and recrystallization of zircon and preservation of monazite in high-grade metamorphism: conventional and in-situ U–Pb isotope, cathodoluminescence and microchemical evidence. Contrib. Mineral. Petrol., 134, 186–201.

SCHMID, S.M., SCHÖNBORN, G. and KISSLING, E. (1996): Geophysical-geological transect and tectonic evolution of the Swiss-Italian Alps. Tectonics, 15, 1036–1064.

SCHMID, S.M. and KISSLING, E. (2000): The arc of the Western Alps in the light of new data on deep crustal structure. Tectonics, 19, 62–85.

SERGEEV, S.A., MEIER, M. and STEIGER, R.H. (1995): Improving the resolution of single-grain U/Pb dating by use of zircon extracted from feldspar: application to the Variscan magmatic cycle in the Central Alps. Earth Planet. Sci. Lett., 134, 37–51.

SEWARD, D. and MANCKTELOW, N.S. (1994): Neogene kinematics of the Central and Western Alps: Evidence from fission-track dating. Geology, 22, 803–806.

STACEY, J.S. and KRAMERS, J.D. (1975): Approximation of terrestrial lead isotope evolution by a two-stage model. Earth Planet. Sci. Lett., 26, 207–221.

STAMPFLI, G.M. (1993): Le Briançonnais, terrain exotique dans les Alpes? Eclogae geol. Helv., 86, 1–45.

STAMPFLI, G.M. (1996): The Intra-Alpine terrain: a Paleotethyan remnant in the Alpine Variscides. Eclogae geol. Helv., 89, 13–42.

STAMPFLI, G.M., MOSAR, J., MARQUER, D., MARCHANT, R., BAUDIN, T. and BOREL, G. (1998): Subduction and obduction processes in the Swiss Alps. Tectonophysics, 296, 159–204.

STEIGER, R.H. and JÄGER, E. (1977): Subcommission on geochronology: Convention on the use of decay constants in geo- and cosmochronology. Earth Planet. Sci. Lett., 36, 359–362.

TERA, F. and WASSERBURG, G.J. (1974): U–Th–Pb systematics on lunar rocks and inferences about lunar evolution and the age of the moon. Proceedings of the 5th Lunar Conference, Geochim. Cosmochim. Acta, 2, 1571–1599.

VAI, G.B. and COCOZZA, T. (1986): Essai de zonation synthétique de la chaîne hercynienne en Italie. Bull. Soc. Géol. France, 8ème série, II, 95–114.

VALVERDE-VAQUERO, P. and DUNNING, G.R. (2000): New U–Pb ages for Early Ordovician magmatism in Central Spain. J. Geol. Soc. London, 157, 15–26.

VEARNCOMBE, J.R. (1983): High pressure-low temperature metamorphism in the Gran Paradiso basement, Western Alps. J. Metamorphic Geol., 1, 103–115.

VON RAUMER, J.F. (1998): The Paleozoic evolution in the Alps: from Gondwana to Pangea. Geol. Rundsch., 87, 407–435.

VON RAUMER, J.F. and NEUBAUER, F. (1993): Late Precambrian and Paleozoic evolution of the alpine basement – an overview. In: VON RAUMER, J. and NEUBAUER, F. (eds): Pre-Mesozoic Geology in the Alps. Springer-Verlag, Berlin, 625–639.

ZIEGLER, P.A. (1993): Late Palaeozoic-Early Mesozoic plate reorganization: evolution and demise of the Variscan fold belt. In: VON RAUMER, J. and NEUBAUER, F. (eds): Pre-Mesozoic Geology in the Alps. Springer-Verlag, Berlin, 203–216.

Manuscript received June 2, 2000: revision accepted September 14, 2000.